DEUTSCHES ELEKTRONEN-SYNCHROTRON DESY

DESY 87-056
June 1987



# NUMERICAL STUDY OF FINITE VOLUME EFFECTS IN THE 4-DIMENSIONAL ISING MODEL

I. Montvay

*Deutsches Elektronen-Synchrotron DESY, Hamburg*

P. Weisz

*II. Institut f. Theor. Physik, Universität Hamburg*

ISSN 0418-9833

NOTKESTRASSE 85 · 2 HAMBURG 52

To be sure that your preprints are promptly included in the
HIGH ENERGY PHYSICS INDEX ,
send them to the following address ( if possible by air mail ) :

DESY
Bibliothek
Notkestrasse 85
2 Hamburg 52
Germany

DESY 87-056
June 1987

ISSN 0418-9833

# Numerical study of finite volume effects in the 4-dimensional Ising model

I. Montvay
Deutsches Elektronen-Synchrotron DESY, Hamburg
P. Weisz*
II. Institut für Theoretische Physik der Universität Hamburg

June 4, 1987

**Abstract**

The effect of the finite lattice size on physical quantities, like masses and coupling constants, is numerically investigated in the 4-dimensional Ising model. The feasibility to obtain numerical information about low energy scattering from finite volume effects in a lattice Monte Carlo calculation is demonstrated.

## 1 Introduction

The numerical investigation of relativistic quantum field dynamics is based on the approximation of the space-time continuum by a 4-dimensional discrete lattice. This approximation becomes good if the physical length scale is much larger than the lattice spacing. Since the number of lattice points is limited by the available computing power, the need to minimize the influence of the space-time discretization necessarily drives the numerical investigations into regions, where the lattice extension is not much larger than the characteristic physical length scale. In this respect the number of dimensions plays a rather negative rôle, because a mere doubling of the linear extensions implies a drastic factor of 16 increase in the number of lattice points. As a consequence, the knowledge and control of finite lattice size effects is very important in every numerical lattice calculation. In fact, an optimal calculation turns the tables and uses the calculated finite size effects to obtain additional dynamical information on the infinite volume system.

Although the question of the finite size effects on masses or coupling constants was considered in many of the numerical investigations of 4-dimensional quantum field systems, the earlier theoretical studies of the finite size effects were mainly oriented by statistical physics considerations, such as phase transitions etc. (see, for instance, Refs. [1,2,3]). From the point of view of the 4-dimensional numerical simulations a very important question is the influence of the finite lattice size on the calculated particle masses. A systematic theoretical study of the finite volume problem was performed in the recent papers by Lüscher [4,5]. In Ref. [4] the volume dependence of single-particle states was considered, whereas Ref. [5] is devoted to the question of 2-particle scattering states in finite volumes. An interesting outcome of these investigations was the relation between the energy shifts of the 2-particle states in a finite box to the elastic scattering amplitude in infinite volume. This relation allows, in principle, to obtain numerical information on the low energy scattering from an accurate study of the volume dependence of 2-particle energy levels.

The main motivation of the present work is to study the feasibility of the numerical calculation of the scattering length by Lüscher's formula [5]. The choice of the particular quantum field theory, where our numerical simulation has been performed, was also influenced by a possible future application to SU(2) Higgs systems, which are physically important for the understanding of the Higgs-sector of the standard model. (For recent numerical studies of the standard SU(2) Higgs model see [6,7] and references therein.) The 4-dimensional Ising model is a limiting case of the 1-component $\phi^4$ model for infinitely strong self-coupling, therefore it has some similar qualitative features as the standard Higgs sector (which is based on a 4-component $\phi^4$ model). The infinite scalar self-coupling ($\lambda \to \infty$) limit is, in fact, also characteristic to the behaviour at $\lambda \simeq O(1)$, even after the introduction of the SU(2) gauge coupling in the Higgs system [6]. From the point of view of our present problems, the triviality of the continuum limit of the $\phi^4$ model is not relevant. We take the non-trivial finite cut-off model as a representative of quantum field systems on a finite 4-dimensional lattice. (For questions of the continuum limit see [8], where also a detailed list of references to earlier work can be found.) Concerning the physical application to the standard Higgs-sector, the finite cut-off lattice models can be considered as approximations to the effective quantum field theory which has, for some physical reasons, also a finite cut-off. The choice of the 4-dimensional Ising model as a testing ground for numerical simulation methods is, of course, also advantageous because of simplicity. We could perform a large number of sweeps (in the order of $10^6 - 10^7$) on a variety of lattices within a reasonable amount of computer time. This allowed an accurate determination of the physical quantities of interest. A last piece of motivation of our investigation of the 4-dimensional 1-component $\phi^4$ model is the fact that, up to now, this simple model received relatively little attention in the numerical simulations. The previous numerical works, we are aware of, were concerned mainly with the questions related to the triviality of the continuum limit [9,10,11] and with the Monte Carlo renormalization group behaviour [12,13]. The masses and couplings were calculated in most cases, by present standards, only with moderate accuracy.

The 4-dimensional Ising model has a critical point at the critical hopping parameter value $\kappa_{cr} \simeq 0.0748$. For $\kappa \geq \kappa_{cr}$ the symmetry $\phi_x \to -\phi_x$ of the action gets spontaneously broken. In the vicinity of the critical point the correlation length $\xi$ (which is the inverse of the mass in lattice units: $\xi = (am)^{-1}$) is very large. The lattice size becomes infinitesimal on the scale of the infinite volume correlation length, therefore near the critical point the finite size effects have to become infinitely large. As a function of $\kappa$ this happens rather suddenly, because $\kappa$ is a "fine tuning parameter" (near $\kappa_{cr}$ $am$ behaves as $\simeq \sqrt{\kappa_{cr} - \kappa}$).

The consequence of the critical behaviour near $\kappa_{cr}$ is:

- For the study of finite size effects on physical quantities, like masses or coupling constants, one has to stay in the region where $z_L \equiv Lm_\infty \simeq O(1)$. (Here $L$ is the linear extension of the lattice and $m_\infty$ is the mass in lattice units in an infinite volume.)
- The region with $z_L \simeq O(1)$ has a very sharp boundary in $\kappa$ due to the fine tuning nature

*Heisenberg foundation fellow

of $\kappa$.

According to this, in our numerical calculations on $L^3 \cdot T$ lattices we kept $z_L$ in the range $z_L \simeq 2-6$ and $z_T \equiv Tm_\infty$ near $z_T \simeq 5-6$. This was achieved by the fine tuning of $\kappa$ in shorter Monte Carlo runs.

The organization of this paper is as follows: in the next Section the lattice definitions of the variables and of the physical quantities are collected. The general formulae for the volume dependence are given in Section 3. In this section also some analytical calculations of the finite lattice size effects in lattice perturbation theory are summarized. In Section 4 the Monte Carlo calculations are described in detail and compared to the theoretical expectations. The last Section contains a short summary and a few concluding remarks.

# 2 Lattice definition of physical quantities

The euclidean lattice action of the 4-dimensional Ising model is defined by

$$S = -\kappa \sum_{x,\mu} \phi_x \phi_{x+\hat{\mu}} \tag{1}$$

Here $\phi_x = \pm 1$ is the field variable at the lattice site $x$, and the summation $\sum_\mu$ goes over $\mu = \pm 1, \pm 2, \pm 3, \pm 4$. $x + \hat{\mu}$ is the neighbouring site to $x$ in the direction $\mu$. The only bare parameter in the action is the (positive) *hopping parameter* $\kappa$. The other parameter of the 1-component $\phi^4$ model, the bare self-coupling $\lambda$, is infinite in the Ising limit. We will work on finite $L^3 \cdot T$ hypercubic lattices with periodic boundary conditions in all directions.

## 2.1 Correlation functions

Let $\mathcal{T}$ denote the transfer matrix in direction 4. $\mathcal{T}$ is positive definite and commutes with the translations $U(\mathbf{a})$ in the spatial directions. For a range of $\kappa$ around the critical point, the theory is thought to describe the interactions of a massive scalar particle. Thus we expect the lowest eigenstates of $\mathcal{T}$ above the ground state [1] to be single particle states with quantized momenta (due to the periodic boundary conditions) $\mathbf{k} = \frac{2\pi}{L}\mathbf{n}$, $\mathbf{n} = (n_1, n_2, n_3)$, $(n_i = integer)$ and energy $\omega(\mathbf{k})$,

$$U(\mathbf{a}) \mid \mathbf{k}\rangle = e^{-i\mathbf{a}.\mathbf{k}} \mid \mathbf{k}\rangle \tag{2}$$

$$\mathcal{T} \mid \mathbf{k}\rangle = e^{-\omega(\mathbf{k})} \mid \mathbf{k}\rangle \tag{3}$$

The physical single particle mass $m(L)$ is given by

$$m(L) = \omega(\mathbf{0}) \tag{4}$$

The energies $\omega(\mathbf{k})$ are determined in the numerical calculations from the 2-point correlations

$$C_1(t_1 - t_2; \mathbf{k}) \equiv \langle S_c(t_1; \mathbf{k}) S_c(t_2; \mathbf{k}) + S_s(t_1; \mathbf{k}) S_s(t_2; \mathbf{k}) \rangle_c \tag{5}$$

of "time-slice" variables with spatial momentum $\mathbf{k}$

$$S_c(t; \mathbf{k}) \equiv \frac{1}{L^3} \sum_{\mathbf{x}} \phi_{\mathbf{x}t} \cos(\mathbf{k}\mathbf{x})$$

[1] $\mathcal{T}$ is normalized so that its largest eigenvalue is 1, i.e. the ground state energy $E_0 = 0$.



$$S_s(t; \mathbf{k}) \equiv \frac{1}{L^3} \sum_{\mathbf{x}} \phi_{\mathbf{x}t} \sin(\mathbf{k}\mathbf{x}) \tag{6}$$

$t$ is the euclidean time $t \equiv x_4$ and $(x_1, x_2, x_3) \equiv \mathbf{x}$ are the spatial components of the site vector $x$. In Eq. (5) $\langle \ldots \rangle_c$ denotes the connected expectation value with respect to the Boltzmann-distribution $e^{-S}$ with the action $S$.

The spectrum of $\mathcal{T}$ also contains states corresponding to scattering 2-particle states with definite total momentum and relative momentum $\mathbf{q}$. To numerically investigate these channels it would, in principle, also be possible to use local 2-particle variables like e. g. $\phi_x^2$, but these would couple only weakly. In order to have a strong overlap with 2-particle states one has to consider variables which are "smeared" in space for fixed time. Good operators, projecting on states with total momentum zero, can be obtained simply by squaring the 1-particle time-slices: [2]

$$S_2(t; \mathbf{q}) = S_c(t; \mathbf{q})^2 + S_s(t; \mathbf{q})^2 \tag{7}$$

The corresponding correlations are denoted by

$$C_2(t_1 - t_2)_{\mathbf{q}_1 \mathbf{q}_2} \equiv \langle S_2(t_1; \mathbf{q}_1) S_2(t_2; \mathbf{q}_2) \rangle_c \tag{8}$$

In the unbroken-symmetry phase, where our Monte Carlo calculations will be performed, there is no mixing between 1-particle and 2-particle states. This is due to the exact symmetry $\phi_x \to -\phi_x$. There is, however, no exactly conserved quantum number which would forbid the mixing of 2-particle operators with different relative momenta $\mathbf{q}$. Consequently, although the various 2-particle states have a large projection in the corresponding diagonal correlations, the off-diagonal correlations with $\mathbf{q}_1 \neq \mathbf{q}_2$ are also non-vanishing. An energy estimate for the different 2-particle states can be obtained by computing the matrix $C_2(t)_{\mathbf{q}_1 \mathbf{q}_2}$ and diagonalizing in $\mathbf{q}_1 \mathbf{q}_2$. We denote the lowest 2-particle energy by $M_0(L)$, the first excited 2-particle energy with unit relative momentum by $M_1(L)$.

## 2.2 Masses

The determination of the low-lying spectrum from the correlation functions would be trivial if the time extension $T$ of the lattice and the statistics would be infinitely large. In real life, for finite $T$ and finite statistics, the situation however is more complicated. Denoting the eigenvectors of the transfer matrix by $\mid n\rangle$ and $E_n$ the corresponding eigenvalues, the two point correlation function of an operator $\mathcal{O}(t)$ defined on one time slice, and its expectation value are given by,

$$\langle \mathcal{O}(t) \mathcal{O}(0)^* \rangle = Z^{-1} \sum_{m,n} e^{-E_n T - t(E_m - E_n)} \mid A_{nm} \mid^2 \tag{9}$$

$$\langle \mathcal{O}(t) \rangle = Z^{-1} \sum_n e^{-E_n T} A_{nn} \tag{10}$$

where

$$Z = \sum_n e^{-E_n T} \tag{11}$$

and

$$A_{mn} = \langle m \mid \mathcal{O}(0) \mid n \rangle \tag{12}$$

[2] To project out the spin 0 part one should sum over rotations of $\mathbf{q}$ ; but we did not do this in our measurements.

The dominant t-dependent contributions for large t comes from the lowest state $r$ for which $A_{0r} \neq 0$. We first note that, due to the periodic boundary conditions, there are also states propagating over the boundary in negative time direction and therefore the exponential time dependence of the correlation functions is modified to a cosh-behaviour. Our main purpose however to recall the well-known relations above is to stress the fact that if $\mathcal{O}$ has non-vanishing expectation value then its connected 2-point function has in general t-independent contributions. In particular for large T the dominant t-independent contribution is given by

$$\mid A_{00} - A_{11} \mid^2 e^{-m(L)T}$$

Therefore the generic behaviour of the correlation functions one has to consider for large $T$ and $t$ is:

$$C^T(t) \simeq c_0 e^{-Tm} + c_1 \left(e^{-tE_r} + e^{-(T-t)E_r}\right) \tag{13}$$

Sometimes the $t$-independent term is known to be absent, e.g. for the 1-particle correlation in the symmetric phase. But for the 2-particle correlations $c_0 \neq 0$. Despite the fact that the $t$-independent terms vanish exponentially for large T, their omission in fits can considerably disturb the determination of the mass: the apparent masses obtained from the logarithmic slope at large $t$ seem to be smaller on the finite-$T$ lattice than for $T \to \infty$.

The behaviour in Eq. (13) is, of course, only the asymptotic form because above the lowest state with energy $E_r$ there are also states with higher energies. In practical calculations one has to extract somehow the lowest contribution, for instance, by fits and/or by some extrapolation procedure. For an accurate calculation the uncertainty of this extrapolation may be comparable to the statistical errors. Therefore it is better to separate this problem from the other sources of errors by defining *effective masses* $\mu_{t_1 t_2} \equiv a m_{t_1 t_2}$ for given pairs $(t_1, t_2)$ of time-slices. In the case of $c_0 = 0$ (no $t$-independent contribution) a simple way to do this is to assume a cosh-behaviour between the two time-slices. The ratio of the correlation function at $t_1$ and $t_2$ is then

$$r_{12} = \frac{e^{-t_1 \mu_{t_1 t_2}} + e^{-(T-t_1)\mu_{t_1 t_2}}}{e^{-t_2 \mu_{t_1 t_2}} + e^{-(T-t_2)\mu_{t_1 t_2}}} \tag{14}$$

The value of $\mu_{t_1 t_2}$ can be obtained, for instance, by numerically solving the equation

$$r_{12}\left(x^{\tau_2} + x^{-\tau_2}\right) = \left(x^{\tau_1} + x^{-\tau_1}\right) \tag{15}$$

with $\tau_i \equiv (\frac{T}{2} - t_i)$ for $x \equiv \exp(-\mu_{t_1 t_2})$. In the case of $c_0 \neq 0$ one can proceed similarly after eliminating the $t$-independent term by subtraction. For instance, for $(t_2 - t_1) \geq 2$ one can take an intermediate time-slice at $t_0 = (t_2 + t_1)/2$ ($t_i$ integer) and solve the equation

$$r_{12}\left(x^{\tau_2} + x^{-\tau_2} - x^{\tau_0} - x^{-\tau_0}\right) = \left(x^{\tau_1} + x^{-\tau_1} - x^{\tau_0} - x^{-\tau_0}\right) \tag{16}$$

The third time-slice $t_0$ can, of course, also be chosen differently, but from the practical point of view it is better to take some definite function of $t_1$ and $t_2$, otherwise the effective mass will already depend on 3 variables $(t_0 t_1 t_2)$.

Another possible way to introduce an effective mass $\mu_{t_1 t_2}$ is to fit the correlation function in the interval $t_1 \leq t \leq t_2$ by the asymptotic form in Eq. (13). This assumes that an error estimate of the correlation function is also available and then it is possible to define $\mu_{t_1 t_2}$ by the minimum of $\chi^2$ (sum of quadratic deviations weighted by the inverse error squares). In



our case it turned out that both methods are practicable and give comparable results. Solving the equations (15) or (16) is, however, simpler. The fit procedure is more cumbersome and numerically more delicate, especially in the case $c_0 \neq 0$.

The question of extrapolating $\mu_{t_1 t_2}$ to the limiting value $\mu$ is, of course, still there. In general they provide upper bounds and in an ideal case $\mu$ can be deduced from the set of obtained $\mu_{t_1 t_2}$ values together with an estimate of the error of this extrapolation.

## 2.3 Off-shell couplings

Information on the physical couplings can be obtained in the symmetric phase from the connected 4-, 6-, etc. point functions. The simplest possibility is to consider the couplings at zero four-momenta, which can be numerically obtained from the *generalized susceptibilities*

$$\chi_n \equiv \frac{1}{L^3 T} \sum_{x_1 \ldots x_n} \langle \phi_{x_1} \ldots \phi_{x_n} \rangle_c \tag{17}$$

The 2-point susceptibility $\chi_2$ plays a special rôle since it defines a dimensionless field renormalization factor $z$ through

$$z(L,T) \equiv (am(L))^2 \chi_2 \tag{18}$$

The multiplicative field renormalization factors in the susceptibilities can be cancelled by taking ratios [7]:

$$a^{4-2n} \Lambda_n \equiv \frac{\chi_n}{(\chi_2)^{\frac{n}{2}}} \tag{19}$$

Here the dimension is indicated by the explicit power of the lattice spacing $a$, therefore a convenient dimensionless combination is:

$$\lambda_n(L,T) \equiv m^{2n-4} \Lambda_n \tag{20}$$

It is also possible to consider off-shell couplings for non-zero euclidean momenta. In the special case of space-like momentum pairs in the 4-point coupling the appropriate generalisation of Eq. (17) is

$$\begin{aligned} \chi_4(\mathbf{k}_1, \mathbf{k}_2) &\equiv \frac{1}{L^3 T} \sum_{x_1 \ldots x_4} e^{i\mathbf{k}_1(\mathbf{x}_1 - \mathbf{x}_2) + i\mathbf{k}_2(\mathbf{x}_3 - \mathbf{x}_4)} \langle \phi_{x_1} \ldots \phi_{x_4} \rangle_c \\ &= \frac{L^9}{T} \sum_{t_1 \ldots t_4} \langle [S_c(t_1;\mathbf{k}_1) S_c(t_2;\mathbf{k}_1) + S_s(t_1;\mathbf{k}_1) S_s(t_2;\mathbf{k}_1)] \\ &\quad [(S_c(t_3;\mathbf{k}_2) S_c(t_4;\mathbf{k}_2) + S_s(t_3;\mathbf{k}_2) S_s(t_4;\mathbf{k}_2)] \rangle_c \end{aligned} \tag{21}$$

In the present paper we shall consider only two cases, namely $\mathbf{k}_1 = \mathbf{1}$, $\mathbf{k}_2 = \mathbf{0}$ and $\mathbf{k}_1 = \mathbf{1}_1$, $\mathbf{k}_2 = \mathbf{1}_2$. Here $\mathbf{1}$ and $\mathbf{1}_1 \neq \mathbf{1}_2$ denote one of the three possible space-like momenta with length $(2\pi)/L$. The corresponding dimensionless couplings can be defined in analogy to Eqs. (19, 20), for instance, as

$$\begin{aligned} \lambda_4(1,0) &\equiv (E_1)^4 \Lambda_4(1,0) \equiv (aE_1)^4 \frac{\chi_4(\mathbf{1},\mathbf{0})}{\chi_2^2} \\ \lambda_4(1,1) &\equiv \frac{(E_1)^8}{m^4} \Lambda_4(1,1) \equiv \frac{(aE_1)^8}{(am)^4} \frac{\chi_4(\mathbf{1}_1,\mathbf{1}_2)}{\chi_2^2} \end{aligned} \tag{22}$$

Here $E_1$ is the energy of the 1-particle state with lowest non-zero momentum. Near the continuum limit and for large volumes it has to satisfy Lorentz-invariance, therefore

$$aE_1 \simeq \sqrt{(am)^2 + \frac{4\pi^2}{L^2}} \tag{23}$$

The non-zero momentum couplings could also be made dimensionless just by the powers of the mass. The advantage of choosing the above combinations of the energy and the mass is that for these definitions the contribution of the 1-particle pole is the same for $\lambda_4$, $\lambda_4(1,0)$ and $\lambda_4(1,1)$. Therefore, the comparison of these couplings directly tells how strong the dominance of the 1-particle pole in the 4-point function is. If $\lambda_4$, $\lambda_4(1,0)$, $\lambda_4(1,1)$ are nearly the same, the common value can also be considered as a good estimate for the on shell coupling.

# 3 Theoretical aspects

## 3.1 Further definitions

In this section we collect some definitions which are required in order to compare the Monte-Carlo results with analytic calculations. [3] For perturbative and other analytic studies it is convenient to work in the $T \to \infty$ limit. The one particle energies $\omega(\mathbf{k})$ then manifest themselves as poles of the $\phi$ - propagator $G(\mathbf{k}, k_4)$ in the complex $k_4$ - plane. Near the pole we have

$$G(\mathbf{k}, k_4) = \frac{Z(\mathbf{k})}{k_4^2 + \omega(\mathbf{k})^2} + O(1) \tag{24}$$

A renormalized mass parameter $m_R(L)$ and a wave function renormalization constant $Z_R(L)$ are usually defined through the behaviour of the inverse propagator for small momenta by [4]

$$G(\mathbf{0}, k_4)^{-1} = 2\kappa Z_R(L)^{-1}(m_R^2 + k_4^2 + O(k_4^4)) \tag{25}$$

The zero momentum wave function renormalization factor $Z_R$ above is related to that defined in Eq. (18) by

$$Z_R(L) = 2\kappa r(L)^2 z(L, \infty) \tag{26}$$

where

$$r(L) = \frac{m_R(L)}{m(L)} \tag{27}$$

The n-point zero momentum couplings in renormalized perturbation theory are conventionally defined [8] by appropriate factors of $Z_R(L)$ times the susceptibilities Eq. (17) and hence are simply related to the dimensionless couplings $\lambda_n$ in Eq. (20) measured in the numerical simulation. In particular for the 4-point coupling $g_R$ and 6-point coupling $h_R$ we have

$$g_R(L) = -r(L)^4 \lambda_4(L, \infty) \tag{28}$$

$$h_R(L) = r(L)^8 \lambda_6(L, \infty) \tag{29}$$

[3] We set the lattice spacing $a = 1$ throughout this section.

[4] The $Z_R$ defined here differs from that defined in [8] by a factor $2\kappa$.



Finally in the infinite volume limit the spectrum becomes continuous and a scattering amplitude can be defined by analytic continuation of the connected amputated 4-point function $\Gamma$,

$$T(\mathbf{p}', \mathbf{q}' \mid \mathbf{p}, \mathbf{q}) = (Z(\mathbf{p}')Z(\mathbf{q}')Z(\mathbf{p})Z(\mathbf{q}))^{\frac{1}{2}} \lim_{\epsilon \to 0} \Gamma(\tilde{\mathbf{p}}', \tilde{\mathbf{q}}', -\tilde{\mathbf{p}}, -\tilde{\mathbf{q}}) \tag{30}$$

where

$$\tilde{k} = (\mathbf{k}, (i - \epsilon)\omega(\mathbf{k}))$$

and energy momentum conservation holds:

$$\mathbf{p} + \mathbf{q} = \mathbf{p}' + \mathbf{q}' \quad (mod\, 2\pi)$$

$$\omega(\mathbf{p}) + \omega(\mathbf{q}) = \omega(\mathbf{p}') + \omega(\mathbf{q}')$$

We can now define an on-shell coupling g by the value of the scattering amplitude at threshold,

$$g = -T(\mathbf{0}, \mathbf{0} \mid \mathbf{0}, \mathbf{0}) \tag{31}$$

In terms of this the s-wave scattering length $a_0$ is given by

$$a_0 = -\frac{m_* g}{32\pi m^2} \tag{32}$$

where $m_*$ is the kinetic mass defined in

$$\omega(\mathbf{k}) = m + \frac{\mathbf{k}^2}{2m_*} + O(\mathbf{k}^4) \tag{33}$$

Here we have denoted the $L = \infty$ mass $m(\infty)$ simply by m and this convention will be adopted for other quantities in the following.

### 3.1.1 $L = \infty$ predictions :

The predictions from the $\kappa$-expansion and renormalization group equation analysis [8] for the main $\kappa$ values measured in our Monte Carlo runs are as follows.

For $\kappa = 0.07102$:

$$m_R = 0.49(2)$$
$$g_R = 41(8)$$
$$Z_R = 6.85(7) \tag{34}$$

For $\kappa = 0.07400$:

$$m_R = 0.21(4)$$
$$g_R = 24(3)$$
$$Z_R = 6.59(8) \tag{35}$$

Some 2-loop perturbative results ($L = \infty$) for the quantities defined in the previous subsection are as follows [8], with $\alpha_R \equiv g_R/(16\pi^2)$:

$$h_R = 10 g_R^2 \left(1 - \frac{3}{4}\alpha_R + \frac{9}{4}\alpha_R^2 + O(g_R^3, m_R^2 g_R)\right) \tag{36}$$

$$g = \frac{m^2}{m_*^2} g_R \left(1 - \alpha_R + 0.927\alpha_R^2 + O(g_R^3, m_R^2 g_R)\right) \tag{37}$$

$$m = 2\log\left((1+\frac{m_R^2}{4})^{\frac{1}{2}} + \frac{m_R}{2}\right)\left(1 - 0.0013\alpha_R^2 + O(g_R^3, m_R^2 g_R)\right) \tag{38}$$

$$m_* = m_R\left(1+\frac{m_R^2}{4}\right)^{\frac{1}{2}}\left(1 - 0.0013\alpha_R^2 + O(g_R^3, m_R^2 g_R)\right) \tag{39}$$

We see that the mass ratio $r(\infty)$ defined in Eq. (27) is approximately 1.01 for $m_R \simeq 0.5$ (the deviation from 1 coming mainly from $O(a^2)$ effects), and approximately 1.002 for $m_R \simeq 0.2$.

## 3.2 Finite volume effects

Formulae for the leading finite volume effects for continuum theories in a box with periodic boundary conditions have been derived by Lüscher for both stable particle masses [4] and for 2-particle masses [5]. [5] Analogous formulae can be derived for the theory with lattice cut-off [14] [6] and also to other quantities such as $g_R(L)$ and $Z_R(L)$. In the following we merely summarize these results together with simple calculations in leading order renormalized perturbation theory in the $\phi^4$ model which, according to the picture elucidated in Ref. [8], should suffice to give a good quantitative description when the bare parameters are such that the model is 'in the scaling region' where the renormalized coupling is sufficiently small.

### 3.2.1 Stable particle mass:

The volume dependence of the physical mass $m(L)$ is due to vacuum polarization effects [4], and is, in the symmetric phase where there is no 3-point coupling, given by

$$m(L) - m = -\frac{3}{2m}\int_{-\pi}^{\pi}\frac{d^3q}{(2\pi)^3 2\omega(\mathbf{q})} e^{-\omega(\mathbf{q})L} T(\mathbf{p},\mathbf{q} \mid \mathbf{p},\mathbf{q}) + \ldots \tag{40}$$

where the momentum $\mathbf{p}$ is given by

$$\mathbf{p} = (\mathrm{im}, 0, 0) \tag{41}$$

The expression (40) neglects higher exponentially damped contributions (indicated by the dots), but includes all lattice artifacts. Extracting the leading behaviour of the integral, by expanding around the saddle point, shows that $m(L)$ approaches its asymptotic value exponentially, with pre-factor proportional to the forward scattering amplitude analytically continued to an unphysical point,

$$m(L) - m = -\frac{3}{4m^2} T(\mathbf{p},0 \mid \mathbf{p},0)\left(\frac{\mathrm{m_*}}{2\pi \mathrm{L}}\right)^{\frac{3}{2}} \mathrm{e}^{-\mathrm{mL}}(1 + \mathrm{O}(\mathrm{L}^{-1})) \tag{42}$$

We see that, due to the repulsive nature of the interaction, in the symmetric phase, the limit is approached from above.

[5] The formulae are proven to all orders of perturbation theory, but are thought to be of more general validity.
[6] We are of course primarily interested in the limit $L \gg \xi \gg a$.



Expanding all quantities occurring in (40) in leading order renormalized perturbation theory one obtains

$$m(L) - m = \frac{3g_R m}{m_*^2}\int_{-\pi}^{\pi}\frac{d^3q}{(2\pi)^3 2\omega_0(\mathbf{q})} e^{-\omega_0(\mathbf{q})L} + O(g_R^2) + \ldots \tag{43}$$

with $\omega_0(\mathbf{q})$ given by

$$\sinh\left(\frac{\omega_0(\mathbf{q})}{2}\right) = (m_R^2 + \hat{\mathbf{q}}^2)^{\frac{1}{2}} \tag{44}$$

where we have introduced the usual notation $\hat{q}_\mu = 2\sin\frac{q_\mu}{2}$. The mass difference can of course be directly calculated in renormalized perturbation theory giving

$$\begin{aligned} m(L) - m &= \frac{m_R}{m_*}(m_R(L) - m_R) + O(g_R^2) \\ &= \frac{g_R}{4m_*}(J_1(m_R, L) - J_1(m_R, \infty)) + O(g_R^2) \end{aligned} \tag{45}$$

where

$$J_n(m_R, L) = \frac{1}{L^3}\sum_{\mathbf{k}}\int_{-\pi}^{\pi}\frac{dk_4}{(2\pi)}(\hat{k}^2 + m_R^2)^{-n} \tag{46}$$

In the latter expression the sum over $\mathbf{k}$ goes over one Brillouin zone. The formula (45), which can easilly be evaluated numerically, is manifestly consistent with (43) and gives an indication of the magnitude of higher exponentially damped terms omitted in the latter.

### 3.2.2 Coupling constant:

$g_R(L)$ also approaches its asymptotic value exponentially, however, from below. A formula obtained using similar methods to those used to derive (40), giving the leading behaviour to all orders of perturbation theory, is

$$g_R(L) - g_R = -9L\int_{-\pi}^{\pi}\frac{d^3q}{(2\pi)^3}\frac{Z(\mathbf{q})^2}{4\omega(\mathbf{q})^2} e^{-\omega(\mathbf{q})L}\Gamma(0,q,0,-q)^2\mid_{q_4=i\omega(\mathbf{q})} + \ldots. \tag{47}$$

and hence

$$g_R(L) - g_R = -\frac{9}{4m^2} Z(\mathbf{0})^2 \Gamma(0,p,-0,p)^2 \left(\frac{m_*}{2\pi L}\right)^{\frac{3}{2}} e^{-mL} L(1 + O(L^{-1})) \tag{48}$$

where the momentum $p$ is given by

$$p = (0, im) \tag{49}$$

This in leading order perturbation theory becomes

$$g_R(L) - g_R = -\frac{9g_R^2}{4m_*^{\frac{1}{2}}}\left(\frac{1}{2\pi L}\right)^{\frac{3}{2}} e^{-mL} L(1 + O(L^{-1})) + O(g_R^3) \tag{50}$$

In comparison, the full result to leading order is

$$g_R(L) - g_R = -\frac{3g_R^2}{2}[J_2(m_R, L) - J_2(m_R, \infty)] + O(g_R^3) \tag{51}$$

Typically one finds that the finite volume effects for $g_R(L)$ are percentually larger than for $m(L)$ and again just including the leading behaviour (50) underestimates the effects.

### 3.2.3 Wave function renormalization constant:

The volume dependence of $Z_R(L)$ is very weak for moderately large $m(L)L$ in the scaling region. In 2-loop renormalized perturbation theory we find

$$\frac{Z_R(L)}{Z_R} - 1 = \frac{g_R^2}{6}(I'(0, m_R, L) - I'(0, m_R, \infty)) + O(g_R^3) \tag{52}$$

with $I'$ defined by

$$I'(p, m_R, L) = \frac{1}{L^6}\sum_{\mathbf{q}}\sum_{\mathbf{q}'}\int_{-\pi}^{\pi}\frac{dq_4}{(2\pi)}\int_{-\pi}^{\pi}\frac{dq_4'}{(2\pi)}(\hat{q}^2 + m_R^2)^{-1}(\hat{q}'^2 + m_R^2)^{-1}\frac{d^2}{2\,dp_4^2}[(q + \widehat{q'} + p)^2 + m_R^2]^{-1} \tag{53}$$

$I'$ can be calculated numerically and it can readily be seen that $Z_R(L)$ attains its asymptotic value from below.

### 3.2.4 2-Particle mass shift:

The shift in the 2-particle mass is due to scattering effects [5] and is given by [7]

$$M_0(L) - 2m(L) = -\frac{4\pi a_0}{m_* L^3}\left(1 + c_1\frac{a_0}{L} + c_2(\frac{a_0}{L})^2\right) + O(L^{-6}) \tag{54}$$

with constants $c_1$ and $c_2$ given by

$$c_1 = -2.837297 \tag{55}$$

$$c_2 = 6.375183 \tag{56}$$

A study of the volume dependence of this shift thus provides direct quantitative information on the physical scattering length $a_0$, the situation being extremely favourable due to the notable feature of Eq. (54) that up to $O(L^{-6})$ only $a_0$ appears. As stated above, for the $\phi^4$ theory in the symmetric phase the interaction is repulsive, hence $a_0 < 0$ and then from (54) follows $M_0(L) - 2m(L) > 0$.

# 4 The Monte Carlo calculation

## 4.1 The Monte Carlo runs

The numerical Monte Carlo calculations were performed partly on a serial coputer (IBM 3084) and partly on a vector machine (CYBER 205 at the Karlsruhe University). Consequently, we had two rather different versions of almost all of our programs. This turned out quite useful for checking possible programming errors. During the updating we stored the spin variables in single bits and used multi-spin coding. However, for the Metropolis hits separate random numbers were generated for every spin, in order to avoid the systematic errors due to the multiple use of random numbers [15]. By comparing the results of the first CYBER run on a $16^3 \cdot 24$ lattice to previous IBM runs we realized the danger of the correlations in the pseudo-random generator in a dramatic way. As it was observed previously [16,17,18], the correlations present in the commonly used pseudo-random number generators can influence

[7] We cite here only the formula for zero relative momentum. For other cases see ref. [5].



the Monte Carlo results considerably if the number of sites is a multiple of a high power of 2, and if in a program the number of generated pseudo-random numbers is an integer multiple of the number of sites. (In a serial program this usually does not happen, because the total number of pseudo-random numbers depends on the acceptance of the hits and hence also on the configuration.) In the first version of our vectorized program we ignored the warning of Refs. [16,17,18], and received wrong results (e.g. the 1-particle mass was about 10% smaller than the value given in Table IIA). After realizing the source of the discrepancy we changed the vectorized program according to the suggestion of Ref. [18]: we left out 1 pseudo-random number after every sweep. In the CYBER program we used most of the time the fast generator of Ref. [19], in the IBM program the NAGLIB routine G05CAE.

In order to fix the $\kappa$-value in the final runs we performed a series of shorter runs on a $12^4$ lattice. The aim was to tune $\kappa$ in the unbroken symmetry phase in such a way that the infinite volume mass be near 0.5, respectively, 0.2. This tuning lead to $\kappa \equiv \kappa_{12} = 0.07102$ for $am \simeq 0.5$, respectively, to $\kappa \equiv \kappa_{24} = 0.074$ for $am \simeq 0.2$. (Actually $\kappa = 0.071$ would be as good as our $\kappa_{12}$, but after having made already some longer run we did not want to change $\kappa$ again.) The time extension $T$ of the lattices was chosen in such a way that the systematic error of the mass determination due to $T < \infty$ could be made sufficiently small (smaller than the statistical errors). In a series of runs for fixed $\kappa$ on $12^4$, $12^3 \cdot 24$ and $12^3 \cdot 36$ lattices the masses were determined and compared with each other. The conclusion was that $T = 12$ is enough for $\kappa = \kappa_{12}$ and $T = 24$ for $\kappa = \kappa_{24}$ (hence the indices of $\kappa$). This means $z_T = Tm \simeq 6$, respectively, $z_T \simeq 5$. For the spatial extension we have chosen $L = 4, 6, 8, 12$ in the first case and $L = 8, 10, 12, 14, 16, 18, 20$ in the second case. (Originally a $24^4$ run was also planned but, unfortunately, this did not fit in our computer budget.)

The masses and couplings were calculated always after every $5^{th}$ sweep. The total number of sweeps per lattice ranged between $10^6$ and $10^7$ (see Table IA,IIA for details). The estimate of the statistical errors was directly done for the time-slice correlation functions (see Eqs. (5-8)) and for the off-shell couplings as defined in Eqs. (20,22). This means that these "primary" quantities were calculated in every bin of the data sequence for bin lengths $2^k$ ($k = 0, 1, 2, \ldots$) and the statistical errors were estimated by the resulting estimates of the standard deviations. For every other quantity (as, for instance, the mass) the statistical error estimates were obtained indirectly by assuming, as a rule, that the directly measured statistical errors are uncorrelated. By this procedure the indirectly calculated errors are most probably overestimated, because the different quantities (like the correlations at different distances or $am$ and $a^{4-2n}\Lambda_n$) are obviously correlated. Therefore in some cases the errors of some quantities were neglected in the calculation of the errors of some function of these quantities. (The way of the statistical error estimate will always be explicitly stated in the tables and figures containing the results.) One way to avoid the uncertainties of the indirect error estimates would be to determine every quantity of interest in every data bin. Another possibility would be to measure also the correlations between the primary quantities and take it into account in the error estimates. (This method was shown to work for the functions of Wilson-loops in the SU(2) Higgs model [20].) Both these ways of improved error estimates are, however, rather cumbersome and require a large amount of additional data handling. Therefore, we decided to pursue our simple method which involves some uncertainty, but it is probably always on the safe side of overestimating rather than underestimating the errors.

Observing the dependence of the error estimates on the bin length it is possible to obtain information on the autocorrelation time for different quantities. As representative examples,

the errors of three different quantities at $\kappa = \kappa_{24}$ and of two quantities at $\kappa = \kappa_{12}$ are shown in Figs. 1A-1E as a function of bin length ($2^{k-1}$ in this case). The saturation of the errors occurs on the $18^3 \cdot 24$ lattice (Figs. 1A-1C) for a bin length $b \simeq 2^9 = 512$, whereas on the smaller lattice ($12^4$, in Fig. 1D-1E) for $b \simeq 2^7 = 128$. [8] Since the measurements were done only after every fifth sweeps, the number of sweeps is 5-times more. This gives for the ratio of the autocorrelation times a factor $\simeq 4$, which is not far away from the expected proportionality to the squares of the correlation lengths (i. e. $\simeq 25/4$).

## 4.2 Results and comparison to the theory

The time-slice correlations and off-shell couplings were calculated in the Monte Carlo runs according to the definitions in Sect. 2. All the correlations could be determined to a good precision, in most cases for every considered time-distance. As a sample case, we include in Table III the correlations at $\kappa_{24}$ on the $18^3 \cdot 24$ lattice. (There are similar tables for every lattice. They are available upon request from the authors.) The masses were determined from the correlations in two different ways: by fitting with the asymptotic form in Eq. (13) for a variety of time intervals and also by solving Eqs. (15-16) for different time-slice pairs. Both procedures allow a reliable and consistent mass estimate because the time dependence for larger time-distances is small (smaller than the quoted statistical error). As an illustration of the second method we show the obtained mass estimates on the $18^3 \cdot 24$ lattice in Fig. 2A-2B, respectively, for the 1-particle and 2-particle mass. The errors on these figures were obtained by considering only the error of the more distant time-slice. In this way the correlation between the different time-slices can be approximately taken into account. As it can be seen from Figs. 2A-B, the mass estimates are practically independent from the chosen distance pair. The summary of the final results for the masses is contained in Tables IA and IIA. The notations are as follows: $a$ is the lattice spacing, $m$ the 1-particle mass, $E_1$ the 1-particle energy with lowest lattice space-like momentum, $M_0$ the 2-particle mass with zero relative momentum and $M_1$ the 2-particle mass with unit relative momentum. The definition of $z$ and $\chi_2$ is given in Eqs. (17,18). The values of the mass and renormalization constant are in good agreement with the theoretical estimates Eqs. (34,35).

The volume dependence of the 1-particle mass is shown in Fig. 3A-B. Also included in these figures are the asymptotic formula in Eq. (43) and the exact 1-loop expression in Eq. (45), for which we used the theoretical estimate $g_R = 41$ and an extrapolated value $am_\infty = 0.4877$ for $\kappa = 0.07102$ and, respectively, the set of values $g_R = 24$, $am_\infty = 0.2130$ for $\kappa = 0.07400$. As one can see, both formulae work well for the largest volumes. For the smaller lattices 1-loop lattice perturbation theory is somewhat better: the asymptotic formula is underestimating the finite size effects, the 1-loop formula is slightly overestimating. The theoretical curves are on safer grounds for $\kappa_{24}$ than for $\kappa_{12}$ because both the higher order perturbative corrections and the lattice artifacts are smaller if $\kappa$ is closer to the critical point. Besides higher orders and lattice artifacts there is also an uncertainty in the values of the parameters of the curves, mainly in the case of the renormalized coupling $g_R$. For this we took the theoretical values from Eq. (34,35) which are consistent with the Monte Carlo results, but $g_R$-values differing by 10-15% would also be possible. This leads to a similar relative uncertainty for the predictions of the mass shift $m(L) - m(\infty)$. In view of this the agreement

[8] Note that, contrary to naive expectation, the bin length at which the errors saturate for a given correlation is practically independent of the time separation ( for fixed $\kappa$ and volume ); compare e.g. Figs. 1A and 1B.



in Figs. 3A-B is quite satisfactory.

The mass extracted from the data on $E_1$ using Eq. (23) is consistent with $m(L)$ for large $L$. We expect that the observed discrepancies at small $L$ are due to finite $a^2$ effects.

As mentioned already in Sect. 3.2.3, the volume dependence of the wave function renormalization constant is very small for the $\kappa$ values we studied. For example for the values $g_R = 24$, $am_\infty = 0.2130$ in Eq (52) we obtain the results $-0.01$, $-0.001$, $-0.0005$ if, respectively, $L = 10, 14, 16$. There is an indication of the expected few percent shift at $L = 8$, but the errors are not small enough. Apart from that our results are consistent with volume insensitivity when $M(L)L > 2$.

For the difference of the lowest 2-particle mass minus twice the 1-particle mass the results are shown by Figs. 4A-B. The continuous curve in these figures is Lüscher's formula Eq. (54), using the same sets of values of $g_R$ and $am$ which were quoted above (and used for Figs. 3A,3B). The corresponding values of the infinite volume scattering length are: $a_0 = -0.64$, respectively, $a_0 = -0.96$. The agreement between the theoretical curve and the Monte Carlo results is impressive. Since $M_0(L) - 2m(L)$ is roughly proportional to the scattering length, its $L$-dependence can be used to determine $a_0$ and the relative error of the result will be essentially given by the relative error of the last points for $M_0(L) - 2m(L)$ where the formula is still valid. With our present errors we could obtain in this way the value of $a_0$ with an error of about $10 - 15\%$.

Unfortunately, the data on the mass difference for the exited 2-particle state $M_1(L) - 2E_1(L)$ is not precise enough to make any useful comparison with the theoretical prediction.

The results for the off-shell couplings are collected in Tables IB and IIB. For the notations see Eqs. (17-22). Besides the 4-point couplings $\lambda_4$, $\lambda_4(1,0)$ and $\lambda_4(1,1)$ the 6-point coupling $\lambda_6$ could also be determined in most of the cases. The errors of the off-shell couplings are, in general, considerably smaller on the small lattices. This is, of course, to be expected, because the difficulty comes from the large cancellations involved in the calculation of connected parts. If the lattice extension is much larger than the correlation length, there are many uncorrelated pieces of the lattice. This makes the required cancellations problematic. Among the 4-point couplings $\lambda_4(1,0)$ seems to be the best from this point of view: it has usually smaller errors, and even the finite size effects are smaller in it than in the other two 4-point couplings. This is the result of a partial cancellation between the finite size effects for the quantity $\Lambda_4(1,0)$ defined in analogy with Eq. (19) and for the energy $E_1$.

Again for large $L$ there is good agreement with the predictions of Eqs. (34,35) (the $L = 20$ result, which is based on comparatively low statistics, is presumably an unfavourable statistical fluctuation). In $\lambda_4$ there are rather strong finite size effects: its value is considerably smaller on the small lattices than the large volume limit. The data is in good semi-quantitative agreement with the perturbative discussion in Sect. 3.2.2 . For example from Eq. (51) we expect for $am \simeq 0.5$ and $g_R = 41$ that $g_R(L) - g_R(\infty)$ takes the values $\simeq -3$, $\simeq -1$, $\simeq -0.3$ for $L = 8, 10, 12$ respectively. For $am \simeq 0.2$ and $g_R = 24$ we expect $g_R(L) - g_R(\infty) \simeq -5$, $\simeq -3$, $\simeq -1.7$ if $L = 14, 16, 18$.

Finally the results on the 6-point coupling are of the same order of magnitude as that obtained from the perturbative calculation Eq. (36), however, the large statistical errors do not permit a more precise statement.

### 4.3 A short excursion in the critical region

As discussed in the introduction, slightly beyond the hopping parameter values we considered up to now the finite lattice size effects become very large. Of course, in a numerical approach one can ignore this and perform calculations in the critical region with a fixed lattice size. In order to see what happens we did a series of runs in the critical region on a $10^4$ lattice, since this lattice size was common to several earlier Monte Carlo calculations [9,10,11]. In particular, we saw the paper [11] during the course of this work. In this paper the possibility of a vanishing wave-function renormalization factor $Z_R \to 0$ was advocated near the critical point. If taken at the face value, this would be in contradiction to our previous results and also to the analysis in Ref. [8].

The theory of the critical behaviour on finite lattices is formulated in [1,2,3,21]. We do not intend to do a complete finite size scaling analysis here, since our main goal is to obtain information on the physical quantities of the infinite volume theory. (For a very recent finite size scaling study see [22].)

Our $10^4$ runs were performed near the infinite volume critical point $\kappa_{cr} \simeq 0.0748$, namely for $0.0745 \leq \kappa \leq 0.0753$. Besides $10^4$ also $10^3 \cdot 16$ or $16^4$ lattices were considered in a few points. The number of sweeps was between 2.5 to 3.0 $\cdot 10^6$ per point. The results confirmed that the wave function renormalization factor $z' \equiv 2\kappa z$ is decreasing in this $\kappa$-interval. At $\kappa = 0.0753$ we obtained $am = 0.1101(19)$ and $z' = 0.827(32)$. The gentle decrease of $z'$ is probably a finite size effect. This expectation is strengthened by the $16^4$ result $z' = 0.957(16)$ at $\kappa = 0.0745$, compared to the $10^4$ number at the same $\kappa$, namely $z' = 0.935(17)$. However, in this $\kappa$-region there might be a substantial difference between $z'$ and $Z_R$. In addition, the time extension of the lattice is by far too small to project out the lowest eigenvalue of the transfer matrix, therefore the result obtained from a fit by the asymptotic formula (13) cannot really be considered to be the "mass".

At $\kappa = 0.0753$ we stopped our systematic runs, because this point is already in the region dominated by the finite volume dynamics of the constant field mode [3,21]. This means that on the finite lattice, for increasing $\kappa$, the correlation length is further increasing due to the oscillation between the two degenerate minima of the effective potential. The field expectation value in a long enough run still averages out to zero. The critical dynamics is characterized by an autocorrelation time which is proportional to the square of the finite volume correlation length [21]: $\tau_L \simeq \xi_L^2$. This behaviour was roughly verified by $10^4$ runs at $\kappa = 0.0755$ and $\kappa = 0.0760$. In this latter point the "mass", obtained from a fit by the large-$t$ asymptotic form, was $am = 0.068(11)$ and the wave function renormalization factor $z' = 0.63(21)$.

In summary, our $10^4$ calculations are in agreement with the decrease of $z'$ in the critical region on this finite lattice. This cannot, however, be interpreted as the vanishing of the infinite volume $Z_R$ and as the failure of the expected 1-loop renormalization group behaviour $Z_R \to 0.97(1)$ [8]. On the contrary, in the region of $z_L \simeq O(1) - O(10)$ the renormalization group scaling behaviour and 1-loop renormalized perturbation theory do describe the finite size effects quite well (see Figs. 3A-B, 4A-B). Note that our results are at infinite bare self-coupling $\lambda$, whereas the calculations in Ref. [11] were performed at finite $\lambda$. However, as we mentioned before, the behaviour at $\lambda = \infty$ is qualitatively rather similar to the situation for $\lambda = O(1)$.



## 5 Summary and conclusions

The control of finite cutoff and finite volume effects is essential in order to extract relevant physical information from any numerical lattice field theory simulation. With respect to the finite volume effects we are potentially in a good situation since for these universal asymptotic formulae are available (for periodic boundary conditions) [4,5]. Although these results are thought to be of general validity, they are so far only proven in the framework of renormalized perturbation theory. The present numerical simulation in the 4-dimensional Ising model is in good agreement with the asymptotic formulae. In particular, the measurement of the finite volume 2-particle energy levels demonstrates the feasibility to obtain valuable numerical information on low energy scattering from the study of finite volume effects.

The Ising model is a limiting case of the $\phi^4$ field theory. The analysis in Ref. [8] of the $\phi^4$ model in the symmetric phase supported the previous conjectures that close to the critical line it describes an effective continuum theory: there exists a "scaling region", roughly characterized by $am < \frac{1}{2}$, where cutoff effects are small. The latter analysis required as input the validity of renormalized perturbation theory in the scaling region which, despite shown to be self-consistent, remains an assumption to be substantiated.

A short summary of our conclusions from the numerical Monte Carlo calculations is as follows:

- The 1-particle mass can be measured with sufficient accuracy to exhibit its expected exponential approach to the asymtotic $L \to \infty$ limit, the asymptotic behaviour setting in for $z_L > 2 - 3$. The absolute magnitude of the effect requires the knowledge of some forward scattering amplitude. Calculations of this in renormalized perturbation theory yield good agreement with the data.

- The extrapolated $L = \infty$ values of various quantities are all consistent with the quantitative results of Ref. [8]. In particular, our data at $\kappa = 0.074$, where the correlation length is approximately 5 lattice units, gives added confidence to the validity of the analysis in [8] for an extreme value of the bare self-coupling at which one might be most suspect.

- The volume dependence of the lowest 2-particle mass is in remarkable agreement with Lüscher's formula. The hope is that, indeed, information on pion-pion scattering lengths can eventually be obtained by measuring the analogous quantity in QCD [5], once the enormous hurdle of finding an efficient fermion simulation method is overcome. For the two measured points the value of the scattering length times the mass was $a_0 m \simeq -0.3$ and, respectively, $a_0 m \simeq -0.2$. Estimates of the physical pion $S$-wave $I = 0$ scattering length, on the other hand, give $a_0^0 m_\pi \simeq 0.2$ [23]. Therefore the percentual effects for a given value of $z_L$ are expected to be quantitatively similar in our simulation and in the physical pion case, the difference being that the asymtotic limit is approached from below there.

- In the Ising model, as mentioned above, finite size effects are reasonably small provided $z_L > 2 - 3$. However, when the correlation length is approximately equal to the size of the lattice enormous finite size effects are known to occur. In particular, the observed decrease [11] of the wave function renormalization constant for fixed lattice size in the

critical region can be understood as a finite size effect, and no significant conclusion about the behaviour of this quantity in the continuum and infinite volume limit can be made therefrom.

It is plausible that the finite volume behaviour in other $\phi^4$-related models, as e. g. Higgs models, are qualitatively similar to the present case. Nevertheless a numerical study of these related models would also be desirable, in particular also in the broken phase where the interaction is attractive and the 3-particle coupling is non-vanishing.

## Acknowledgements

It is a pleasure to thank Martin Lüscher for discussions and for his constant interest in this work. His important contributions during the first stages of this project considerably influenced the final content of the paper. Finally we would like to thank Paul Weber and Klaus Geers at the Karlsruhe Rechenzentrum for frequent kind assistance with problems we encountered using the CYBER 205.



## References

[1] M. E. Fisher, in *Critical Phenomena,* Proceedings of the 51$^{th}$ Enrico Fermi Summer School, Varena, ed. M. S. Green, Academic Press, New York 1972

[2] M. N. Barber, in *Phase transitions and critical phenomena,* Vol. 8, ed. C. Domb, J. L. Lebowitz, London, Academic Press 1983

[3] E. Brézin, J. Zinn-Justin, Nucl. Phys. **B257** [FS14], (1985) 867

[4] M. Lüscher, in *Progress in Gauge Field Theory,* ed. G. 't Hooft et al., Cargese lectures 1983, Plenum Press 1984; Commun. Math. Phys. **104** (1986) 177

[5] M. Lüscher, Commun. Math. Phys. **105** (1986) 153

[6] I. Montvay, Nucl. Phys. **B269** (1986) 170

[7] W. Langguth, I. Montvay, P. Weisz, Nucl. Phys. **B277** (1986) 11

[8] M. Lüscher, P. Weisz, DESY preprint 87-017 (1987)

[9] B. Freedman, P. Smolensky, D. Weingarten, Phys. Lett. **113B** (1982) 481

[10] I. A. Fox, I. G. Halliday, Phys. Lett. **159B** (1985) 148

[11] K. Huang, E. Manousakis, J. Polonyi, MIT preprint CTP-1420 (1986)

[12] D. J. E. Callaway, R. Petronzio, Phys. Lett. **139B** (1984) 189; Nucl. Phys. **B240** [FS12] (1984) 577

[13] C. B. Lang, Phys. Lett. **155B** (1985) 399; Nucl. Phys. **B265** [FS15] (1986) 630

[14] G. Münster, Nucl. Phys. **B249** (1985) 659

[15] G. Bhanot, D. Duke, R. Salvador, Journ. Stat. Phys. **44** (1986) 985

[16] G. Kalle, S. Wansleben, Computer Phys. Comm. **33** (1984) 343

[17] G. Parisi, F. Rapuano, Phys. Lett. **157B** (1985) 301

[18] T. Filk, K. Fredenhagen, M. Marcu, Phys. Lett. **165B** (1985) 125

[19] W. Celmaster, K. Moriarty, Journal of Comp. Phys. **64** (1986) 271

[20] W. Langguth, I. Montvay, DESY preprint 87-020 (1987)

[21] J. C. Niel, J. Zinn-Justin, Nucl. Phys. **B280** [FS18] (1987) 355

[22] E. Sánchez-Velasco, Cornell preprint, CLNS-87/57 (1987)

[23] J. Gasser, H. Leutwyler, Ann. Phys. **158** (1984) 142

## Table IA

The number of sweeps $Ms$ (in units of $10^6$) and the results for the masses at $\kappa = 0.07102$ on $L^3 \cdot 12$ lattices. The statistical error estimates in the last numerals are given in parentheses. The error estimates for the masses were obtained from fits with the asymptotic behaviour Eq. (13) by assuming that the measured statistical errors of the time-slice correlations at different distances are uncorrelated. The statistical error of $\chi_2$ was determined directly by binning. For $z$ the error of $\chi_2$ and $am$ were taken as uncorrelated.

| $L$ | $Ms$ | $am$ | $aE_1$ | $aM_0$ | $aM_0 - 2am$ | $aM_1$ | $\chi_2$ | $z$ |
|---|---|---|---|---|---|---|---|---|
| 4 | 10.1 | 0.5621(5) | 1.414(2) | 1.330(7) | 0.206(8) | 3.0(3) | 20.90(2) | 6.60(2) |
| 6 | 5.2 | 0.5000(12) | 1.070(2) | 1.096(6) | 0.096(7) | 2.2(2) | 26.47(3) | 6.62(4) |
| 8 | 2.5 | 0.4945(9) | 0.8844(17) | 1.015(8) | 0.026(9) | 1.87(12) | 27.69(6) | 6.77(4) |
| 12 | 10.1 | 0.4875(5) | 0.7011(4) | 0.983(4) | 0.008(5) | 1.43(5) | 28.20(3) | 6.70(2) |

## Table IB

The results for the off-shell couplings at $\kappa = 0.07102$ on $L^3 \cdot 12$ lattices. The statistical error estimates in the last numerals are given in parentheses. The error estimates for $a^{4-2n}\Lambda_n$ were obtained directly by binning. Those for the $\lambda$'s were calculated from the error of the $\Lambda$'s alone, by neglecting the errors of the mass (or energy). Otherwise the errors of the $\lambda$'s would be strongly overestimated due to the obvious correlations between these quantities.

| $L$ | $-a^{-4}\Lambda_4$ | $-\lambda_4$ | $-a^{-4}\Lambda_4(1,0)$ | $-\lambda_4(1,0)$ | $-a^{-4}\Lambda_4(1,1)$ | $-\lambda_4(1,1)$ | $\lambda_6 \cdot 10^{-3}$ |
|---|---|---|---|---|---|---|---|
| 4 | 279(2) | 27.9(2) | 8.30(8) | 33.2(3) | 0.17(1) | 26.7(1.6) | 5.08(8) |
| 6 | 543(10) | 33.9(6) | 29.4(6) | 38.5(8) | 0.65(9) | 17.9(2.5) | 8.78(5) |
| 8 | 644(38) | 38.5(2.3) | 64.4(2.8) | 39.4(1.7) | 3.3(6) | 21(5) | 8(3) |
| 12 | 748(75) | 42.2(4.3) | 169(9) | 40.8(2.2) | 41(3) | 43(4) | 30(20) |



## Table IIA

The same as Table IA, for $\kappa = 0.074$ on $L^3 \cdot 24$ lattices.

| $L$ | $Ms$ | $am$ | $aE_1$ | $aM_0$ | $aM_0 - 2am$ | $aM_1$ | $\chi_2$ | $z$ |
|---|---|---|---|---|---|---|---|---|
| 8 | 3.1 | 0.2452(8) | 0.786(2) | 0.586(4) | 0.096(5) | 1.7(1) | 105.7(3) | 6.36(6) |
| 10 | 3.0 | 0.2293(7) | 0.649(2) | 0.520(3) | 0.061(4) | 1.34(3) | 122.5(3) | 6.44(6) |
| 12 | 4.8 | 0.2231(6) | 0.557(1) | 0.479(3) | 0.033(4) | 1.16(5) | 131.8(4) | 6.56(6) |
| 14 | 5.2 | 0.2168(5) | 0.491(1) | 0.460(3) | 0.026(4) | 1.03(4) | 137.7(3) | 6.47(5) |
| 16 | 2.4 | 0.2142(7) | 0.4427(5) | 0.452(4) | 0.024(5) | 0.91(3) | 140.1(3) | 6.43(7) |
| 18 | 4.9 | 0.2144(5) | 0.4063(6) | 0.440(3) | 0.011(4) | 0.84(3) | 141.1(4) | 6.48(5) |
| 20 | 1.6 | 0.2125(10) | 0.374(1) | 0.432(5) | 0.007(6) | 0.78(4) | 142.6(8) | 6.44(10) |

## Table IIB

The same as Table IIA, for $\kappa = 0.074$ on $L^3 \cdot 24$ lattices. Here the values in the second and last columns are multiplied by a scale factor $S = 10^{-3}$.

| $L$ | $-a^{-4}\Lambda_4 \cdot S$ | $-\lambda_4$ | $-a^{-4}\Lambda_4(1,0)$ | $-\lambda_4(1,0)$ | $-a^{-4}\Lambda_4(1,1)$ | $-\lambda_4(1,1)$ | $\lambda_6 \cdot S$ |
|---|---|---|---|---|---|---|---|
| 8 | 4.61(8) | 16.7(3) | 64.7(1.6) | 24.8(6) | 0.56(13) | 23(5) | 1.83(6) |
| 10 | 7.1(2) | 19.6(6) | 144(4) | 25.4(7) | 2.8(5) | 32(6) | 2.8(2) |
| 12 | 9.1(2) | 22.5(5) | 276(8) | 26.6(8) | 7.5(9) | 28(3) | 4.0(2) |
| 14 | 10.2(4) | 22.5(9) | 483(16) | 28.0(9) | 18.6(2.2) | 28(3) | 4.3(5) |
| 16 | 12.6(1.0) | 26.5(2.1) | 713(48) | 27.4(1.8) | 49(7) | 34(5) | 7(2) |
| 18 | 10.8(1.0) | 22.8(2.1) | 1026(56) | 28.0(1.5) | 92(10) | 32(4) | 4(2) |
| 20 | 18(2) | 36(5) | 1370(160) | 27(3) | 119(35) | 23(7) | 15(8) |

# Table III

Time-slice correlations on $18^3 \cdot 24$ lattice at $\kappa = 0.074$. The first column is the time-slice distance $t$. The second column is the 1-particle correlation, the third and fourth are, respectively, the two-particle correlations with relative momentum 0 and 1, the fifth column is the off-diagonal correlation of two-particle states and the sixth one is the 1-particle correlation with lowest non-zero lattice momentum. The last two columns are obtained from columns 3-5 by diagonalization.

| | | | | | | | |
|---|---|---|---|---|---|---|---|
| 0 | 2.617E-03 | 1.326E-05 | 5.197E-06 | -6.168E-07 | 1.344E-03 | 1.327E-05 | 5.185E-06 |
| | ± 3.4E-06 | ± 3.5E-08 | ± 3.1E-09 | ± 5.2E-09 | ± 5.5E-07 | ± 3.6E-08 | ± 3.6E-08 |
| 1 | 2.117E-03 | 8.570E-06 | 2.256E-06 | -4.994E-07 | 8.953E-04 | 8.580E-06 | 2.246E-06 |
| | ± 3.4E-06 | ± 3.5E-08 | ± 3.1E-09 | ± 5.2E-09 | ± 5.5E-07 | ± 3.6E-08 | ± 3.6E-08 |
| 2 | 1.716E-03 | 5.561E-06 | 9.815E-07 | -3.659E-07 | 5.966E-04 | 5.568E-06 | 9.742E-07 |
| | ± 3.3E-06 | ± 2.3E-08 | ± 1.7E-09 | ± 3.8E-09 | ± 5.0E-07 | ± 2.3E-08 | ± 2.3E-08 |
| 3 | 1.394E-03 | 3.628E-06 | 4.277E-07 | -2.558E-07 | 3.978E-04 | 3.633E-06 | 4.226E-07 |
| | ± 3.3E-06 | ± 2.3E-08 | ± 1.7E-09 | ± 3.8E-09 | ± 5.0E-07 | ± 2.3E-08 | ± 2.3E-08 |
| 4 | 1.130E-03 | 2.392E-06 | 1.867E-07 | -1.733E-07 | 2.652E-04 | 2.395E-06 | 1.833E-07 |
| | ± 3.1E-06 | ± 1.5E-08 | ± 1.4E-09 | ± 3.5E-09 | ± 4.3E-07 | ± 1.6E-08 | ± 1.6E-08 |
| 5 | 9.311E-04 | 1.595E-06 | 8.178E-08 | -1.171E-07 | 1.770E-04 | 1.597E-06 | 7.952E-08 |
| | ± 3.1E-06 | ± 1.5E-08 | ± 1.4E-09 | ± 3.5E-09 | ± 4.3E-07 | ± 1.6E-08 | ± 1.6E-08 |
| 6 | 7.721E-04 | 1.084E-06 | 3.535E-08 | -7.717E-08 | 1.184E-04 | 1.085E-06 | 3.393E-08 |
| | ± 2.9E-06 | ± 1.0E-08 | ± 1.4E-09 | ± 3.7E-09 | ± 3.8E-07 | ± 1.1E-08 | ± 1.1E-08 |
| 7 | 6.515E-04 | 7.565E-07 | 1.608E-08 | -5.299E-08 | 7.966E-05 | 7.574E-07 | 1.513E-08 |
| | ± 2.9E-06 | ± 1.0E-08 | ± 1.4E-09 | ± 3.7E-09 | ± 3.8E-07 | ± 1.1E-08 | ± 1.1E-08 |
| 8 | 5.529E-04 | 5.459E-07 | 8.044E-09 | -3.694E-08 | 5.418E-05 | 5.465E-07 | 7.410E-09 |
| | ± 2.8E-06 | ± 9.0E-09 | ± 1.3E-09 | ± 3.5E-09 | ± 4.0E-07 | ± 9.7E-09 | ± 9.7E-09 |
| 9 | 4.784E-04 | 4.154E-07 | 3.651E-09 | -2.755E-08 | 3.777E-05 | 4.159E-07 | 3.191E-09 |
| | ± 2.8E-06 | ± 9.0E-09 | ± 1.3E-09 | ± 3.5E-09 | ± 4.0E-07 | ± 9.7E-09 | ± 9.7E-09 |
| 10 | 4.334E-04 | 3.377E-07 | 2.770E-09 | -2.174E-08 | 2.758E-05 | 3.381E-07 | 2.418E-09 |
| | ± 2.8E-06 | ± 9.1E-09 | ± 1.4E-09 | ± 4.0E-09 | ± 4.6E-07 | ± 1.0E-08 | ± 1.0E-08 |
| 11 | 4.078E-04 | 2.940E-07 | 3.499E-09 | -1.914E-08 | 2.212E-05 | 2.943E-07 | 3.184E-09 |
| | ± 2.8E-06 | ± 9.1E-09 | ± 1.4E-09 | ± 4.0E-09 | ± 4.6E-07 | ± 1.0E-08 | ± 1.0E-08 |
| 12 | 3.987E-04 | 2.803E-07 | 4.061E-09 | -1.929E-08 | 2.040E-05 | 2.806E-07 | 3.725E-09 |
| | 2.9E-06 | ± 1.0E-08 | ± 1.7E-09 | ± 4.5E-09 | ± 5.0E-07 | ± 1.1E-08 | ± 1.1E-08 |



# Figure captions

**Fig. 1A.** The dependence of the error estimate on the bin length $2^{k-1}$ for the 1-particle correlation at time-slice distance $t = 2$. The lattice is $18^3 \cdot 24$ at $\kappa = 0.074$.

**Fig. 1B.** The same as Fig. 1A, for $t = 10$.

**Fig. 1C.** The same as Fig. 1A, for the 4-point coupling at zero momentum.

**Fig. 1D.** The same as Fig. 1A, for the 1-particle correlation at distance $t = 4$ on $12^4$ lattice at $\kappa = 0.07102$.

**Fig. 1E.** The same as Fig. 1A, for the 4-point coupling at zero momentum on $12^4$ lattice at $\kappa = 0.07102$.

**Fig. 2A.** The 1-particle mass estimates on $18^3 \cdot 24$ lattice obtained by solving Eq. (15) for different time-slice pairs. On the horizontal axis the first time-slice distance is given. Identical symbols belong to same diferences of the time-slice distance. The horizontal line is the final mass estimate.

**Fig. 2B.** The 2-particle mass estimates on $18^3 \cdot 24$ lattice obtained by solving Eq. (16) for different time-slice pairs $(t_1, t_2)$. The third time-slice is $t_0 = (t_1 + t_2)/2$, $(integer)$. On the horizontal axis the first time-slice distance is given. Identical symbols belong to same diferences of the time-slice distance. The horizontal line is the final mass estimate.

**Fig. 3A.** The dependence of the 1-particle mass on the spatial extension $L$ of the $L^3 \cdot 12$ lattice at $\kappa = 0.07102$. The Monte Carlo results are the open circles with error-bars. The dotted horizontal line is the asymptotic value for infinite volume. The full line is the asymptotic formula for $z_L >> 1$ in the form Eq. (42), the dashed line is the 1-loop asymptotic form Eq. (43). The full dots give the full 1-loop perturbative result in Eq. (45).

**Fig. 3B.** The same as Fig. 3A on the $L^3 \cdot 24$ lattice at $\kappa = 0.074$.

**Fig. 4A.** The difference of the 2-particle mass minus twice the 1-particle mass as a function of the spatial extension $L$ of the $L^3 \cdot 12$ lattice at $\kappa = 0.07102$. The line is Lüscher's formula Eq. (54) for a scattering length $a_0 = -0.64$.

**Fig. 4B.** The difference of the 2-particle mass minus twice the 1-particle mass as a function of the spatial extension $L$ of the $L^3 \cdot 24$ lattice at $\kappa = 0.074$. The line is Lüscher's formula Eq. (54) for a scattering length $a_0 = -0.96$.

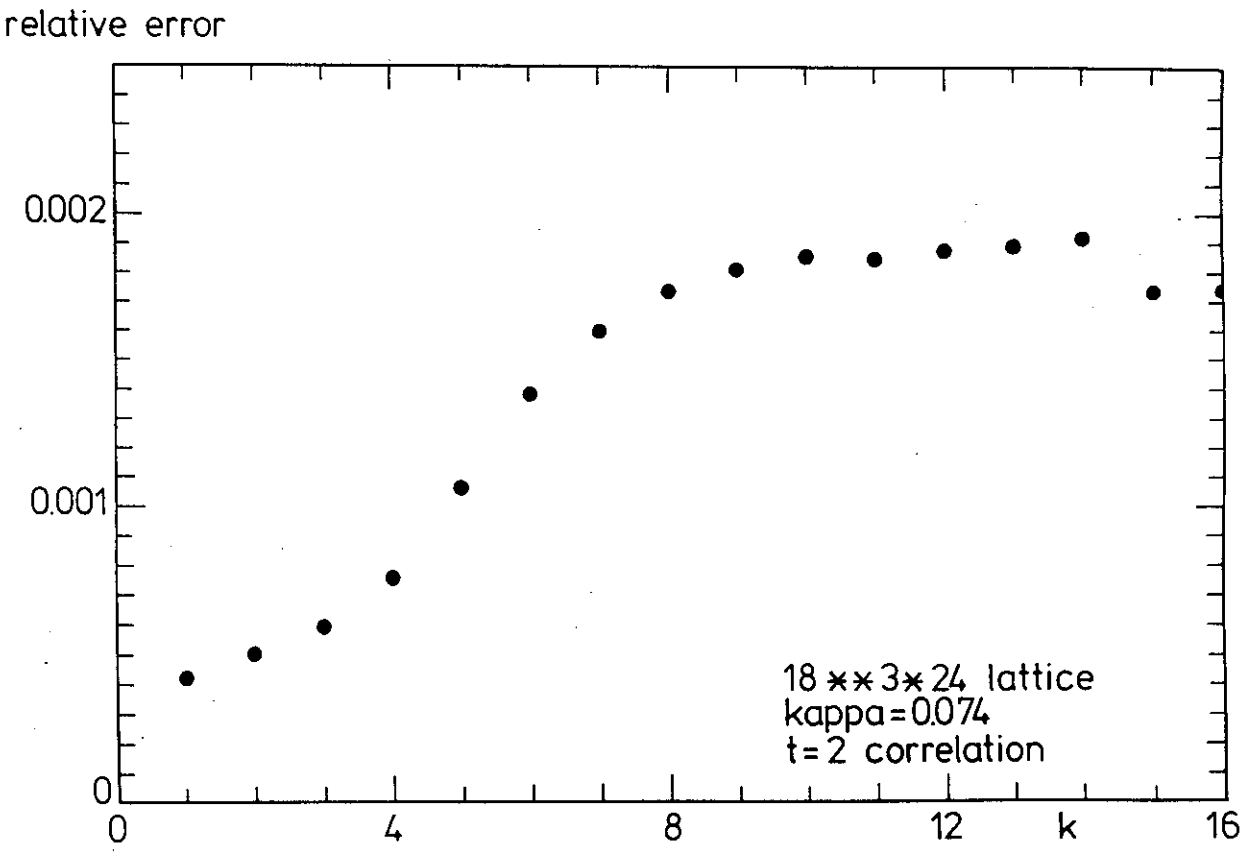
relative error
0.002
0.001
0
0
4
8
12
k
16
18 ** 3* 24 lattice
kappa = 0.074
t = 2 correlation

Fig. 1A

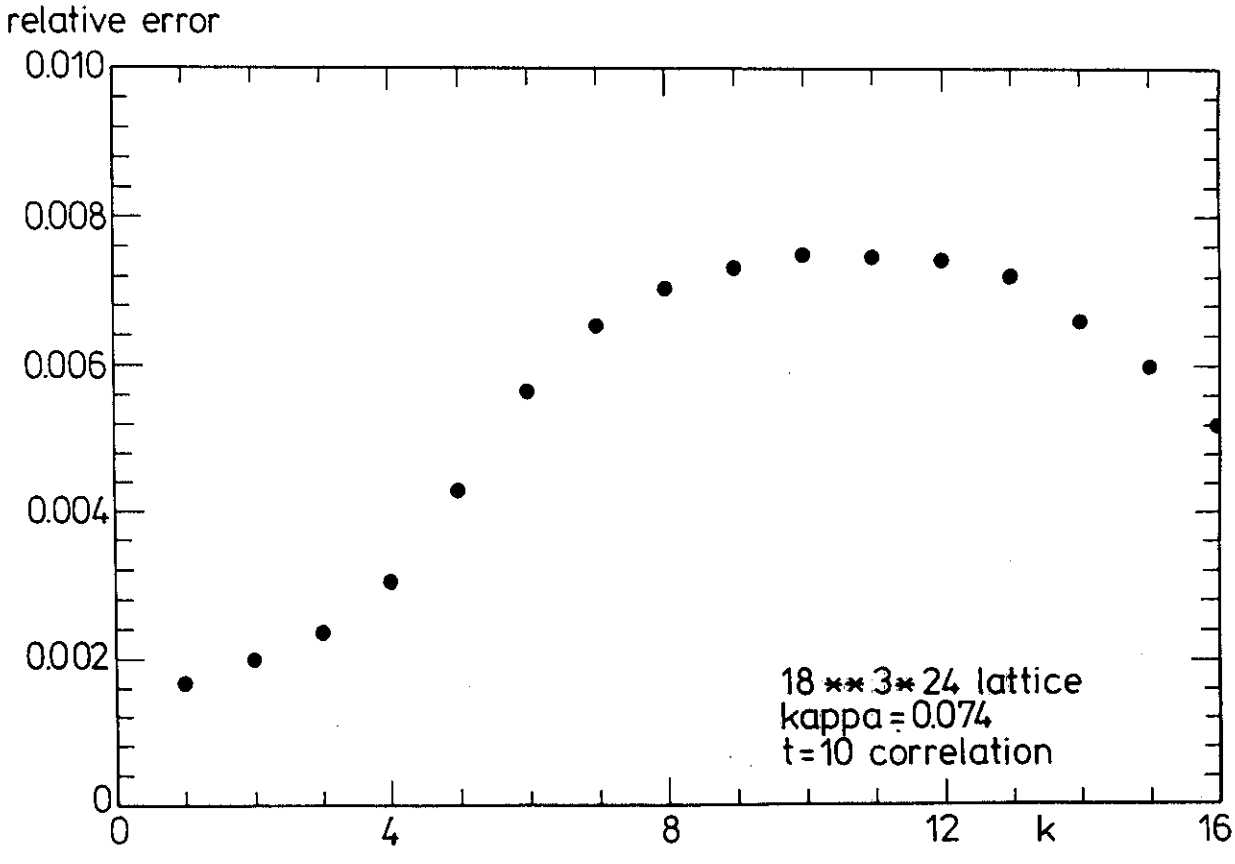
relative error
0.010
0.008
0.006
0.004
0.002
0
0
4
8
12
k
16
18 ** 3* 24 lattice
kappa = 0.074
t = 10 correlation

Fig. 1B

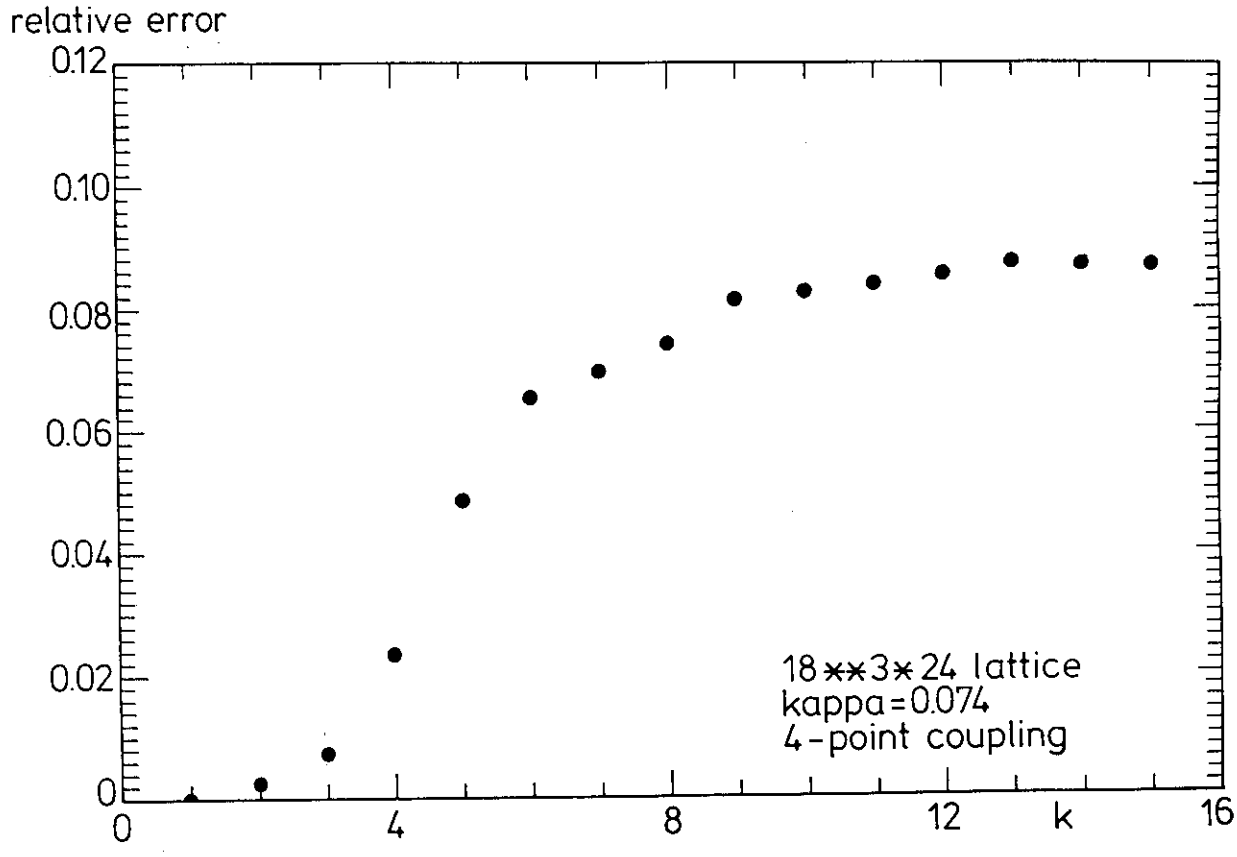
relative error
0.12
0.10
0.08
0.06
0.04
0.02
0
0
4
8
12
k
16
18**3*24 lattice
kappa=0.074
4-point coupling

Fig. 1C

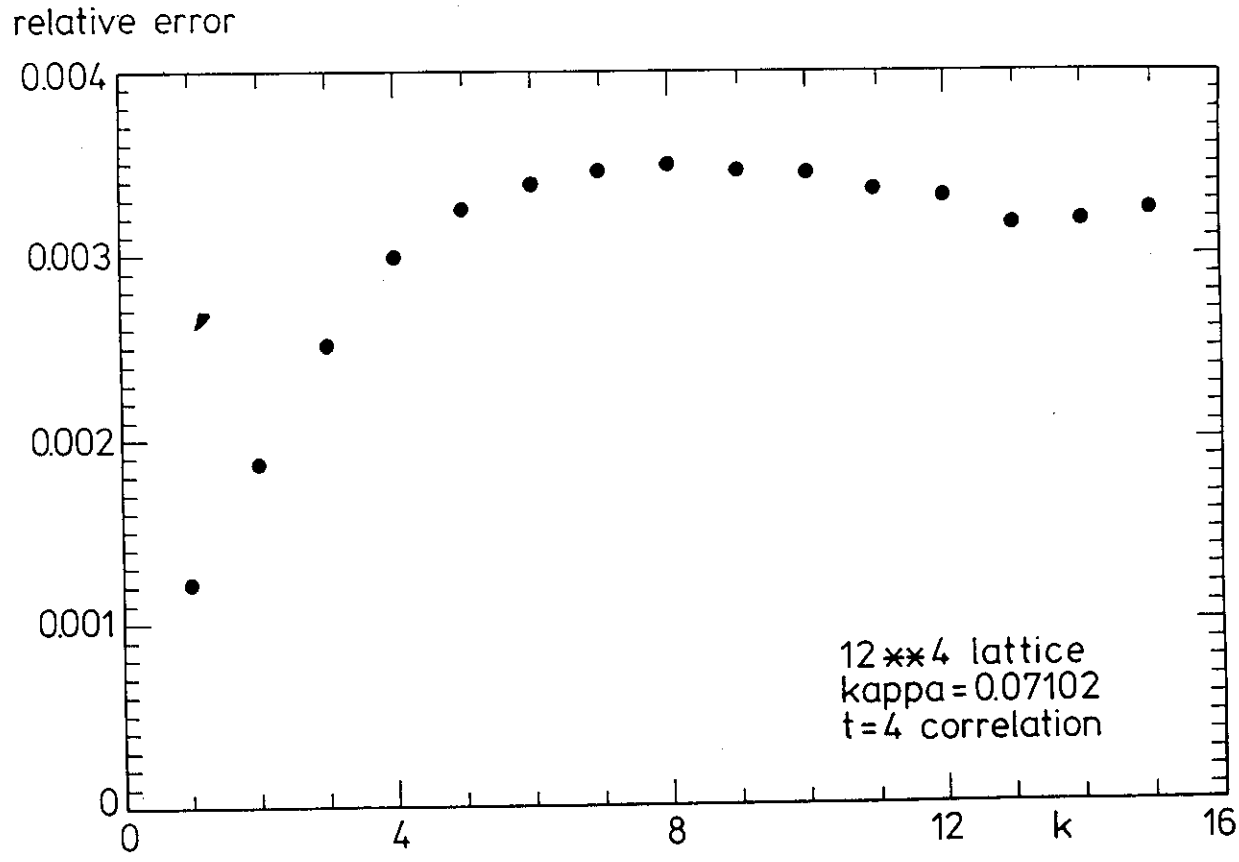
relative error
0.004
0.003
0.002
0.001
0
0
4
8
12
k
16
12**4 lattice
kappa=0.07102
t=4 correlation

Fig. 1D

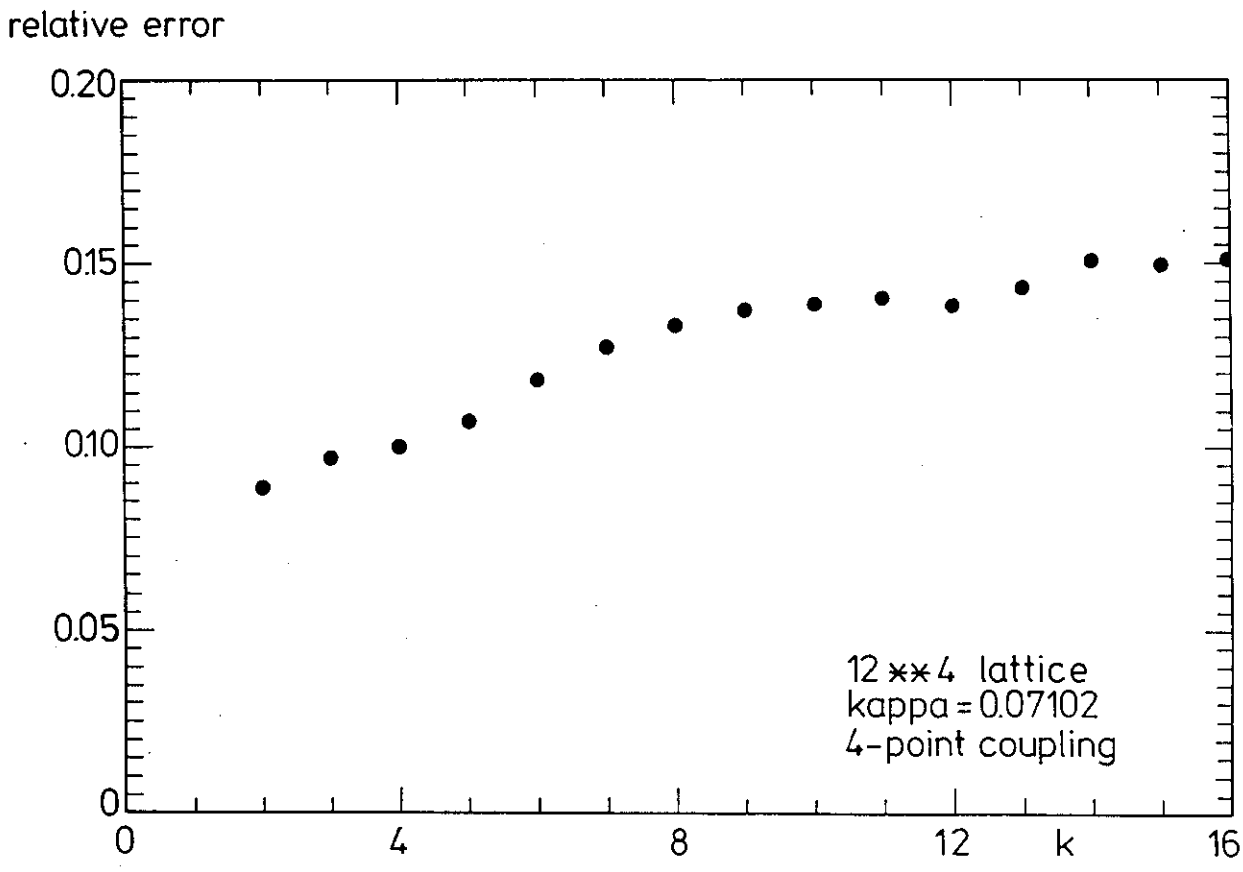
relative error
0.20
0.15
0.10
0.05
0
0
4
8
12
k
16
12 ** 4 lattice
kappa = 0.07102
4-point coupling

Fig. 1E

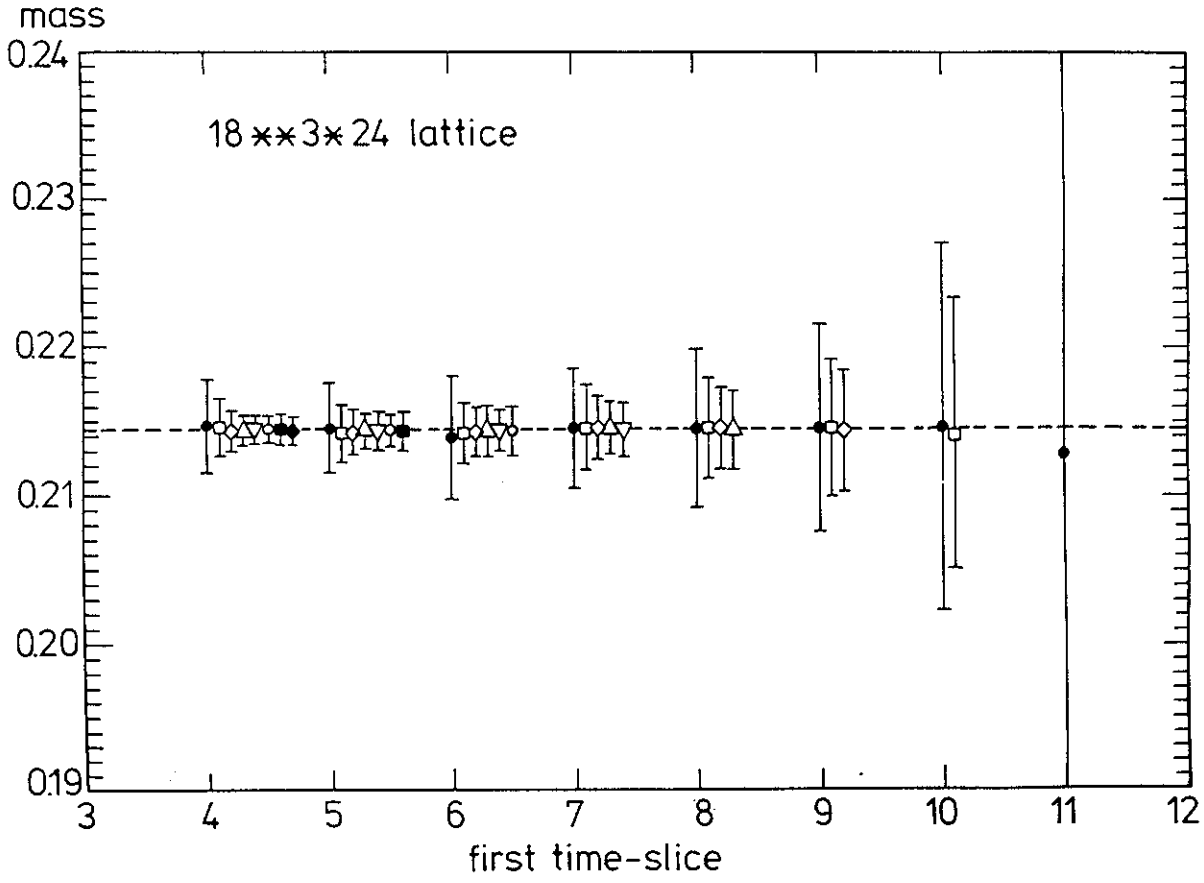
mass
0.24
0.23
0.22
0.21
0.20
0.19
18 ** 3 * 24 lattice
3
4
5
6
7
8
9
10
11
12
first time-slice

Fig. 2A

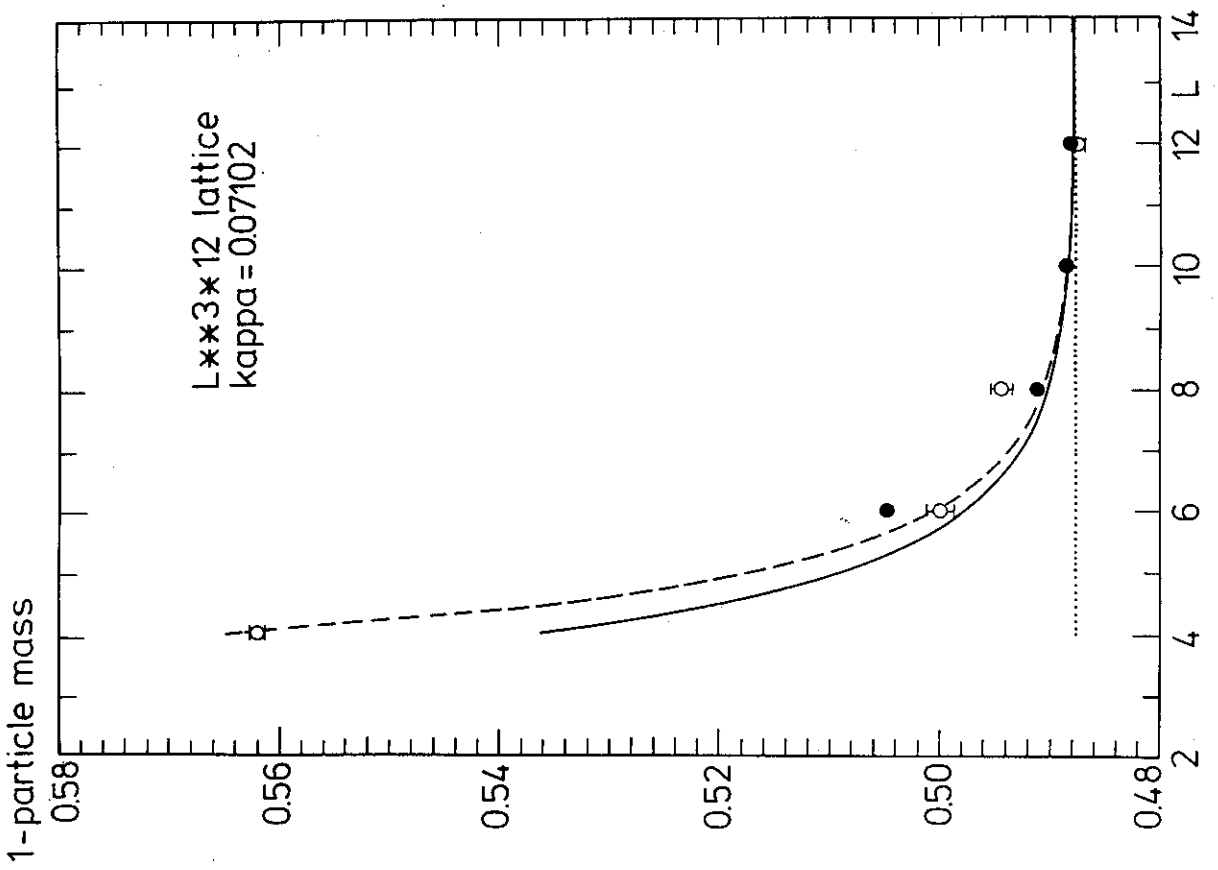
L**3*12 lattice
kappa=0.07102
1-particle mass
0.58
0.56
0.54
0.52
0.50
0.48
2
4
6
8
10
12
14
L

Fig. 3A

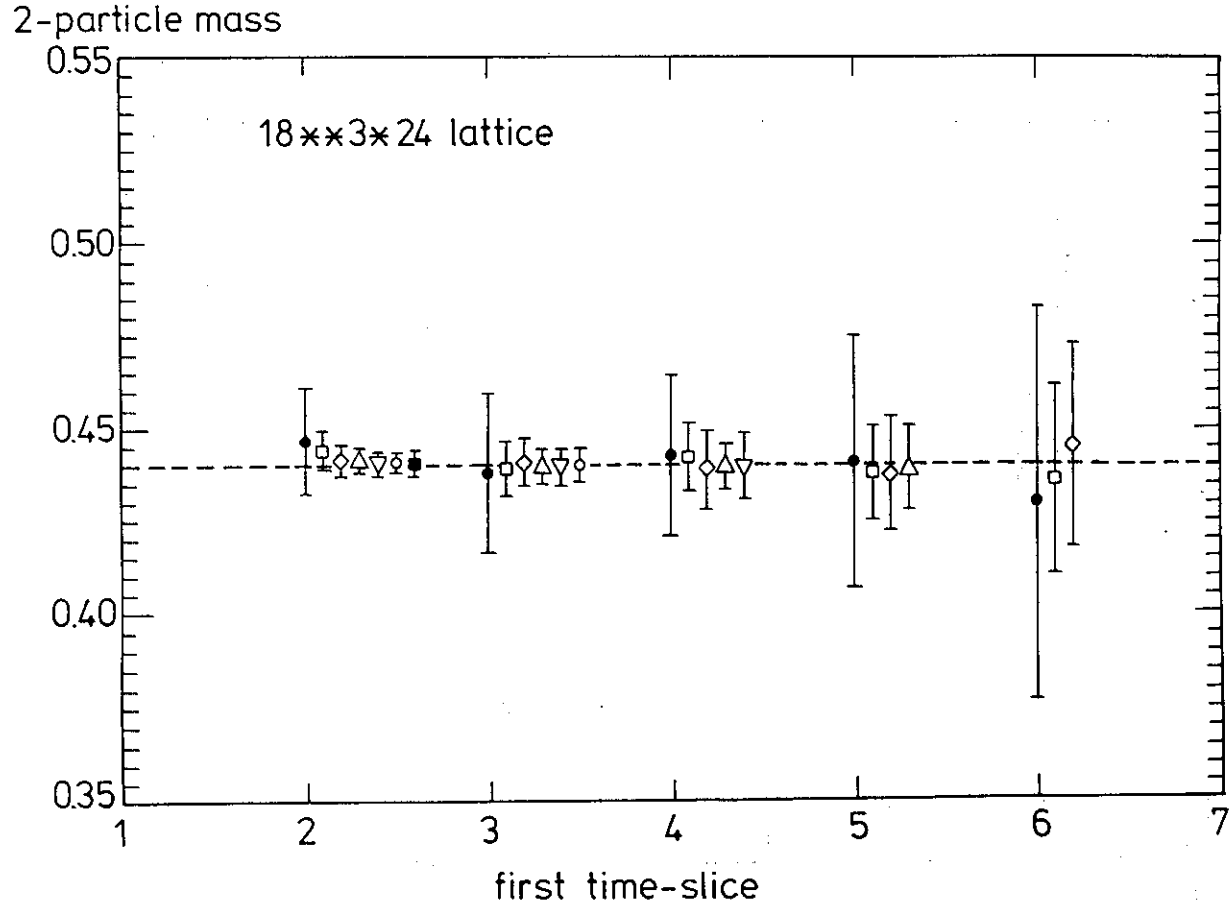
2-particle mass
18**3*24 lattice
0.55
0.50
0.45
0.40
0.35
1
2
3
4
5
6
7
first time-slice

Fig. 2B

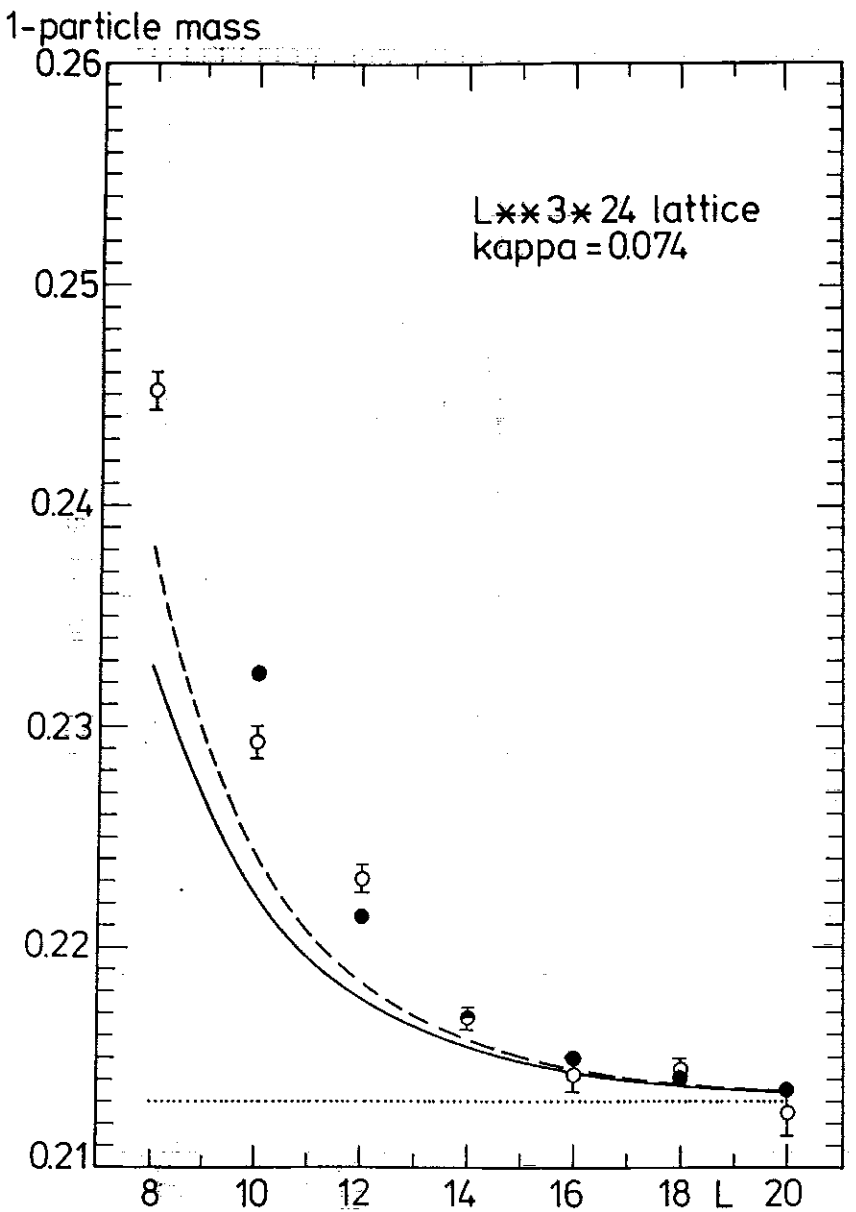
1-particle mass
L**3*24 lattice
kappa = 0.074
0.26
0.25
0.24
0.23
0.22
0.21
8
10
12
14
16
18
L
20

Fig. 3B

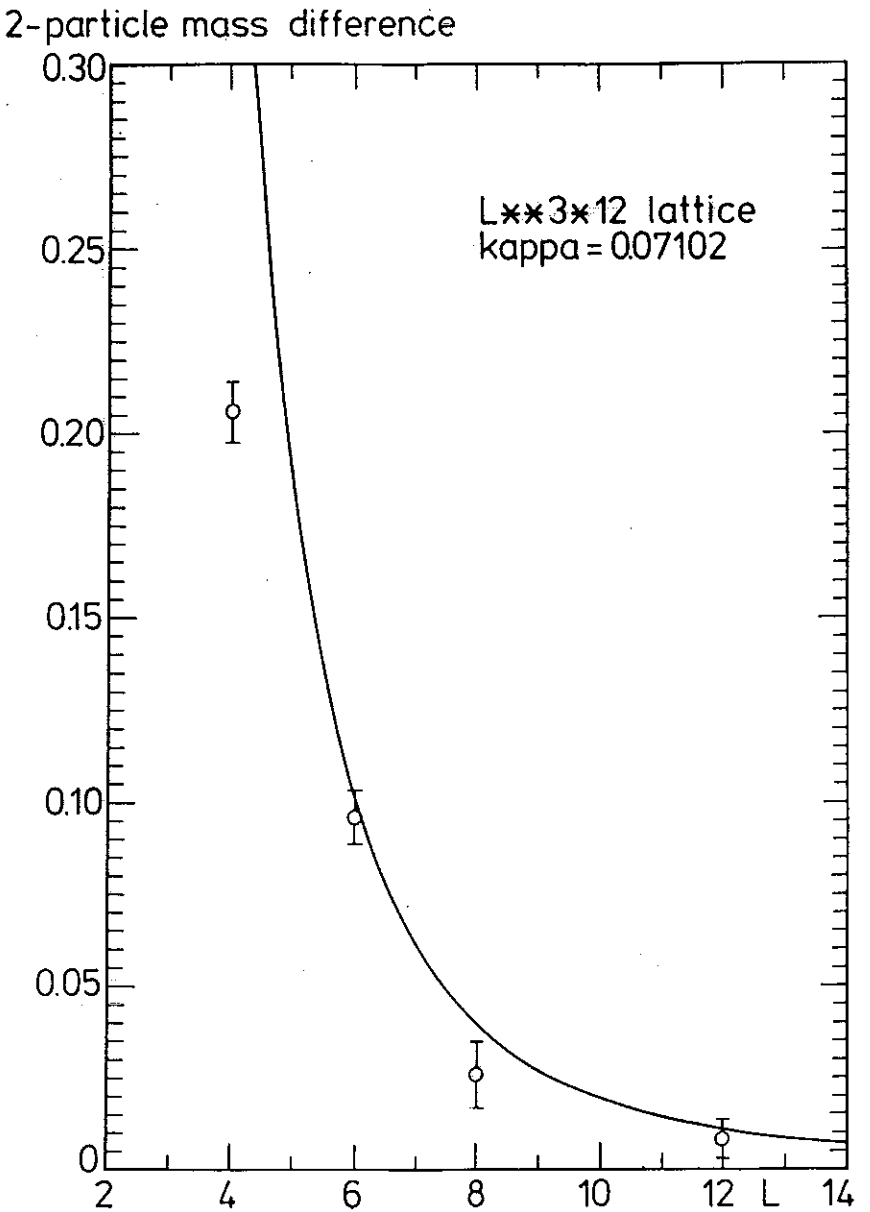
2-particle mass difference
L**3*12 lattice
kappa = 0.07102
0.30
0.25
0.20
0.15
0.10
0.05
0
2
4
6
8
10
12
L
14

Fig. 4A

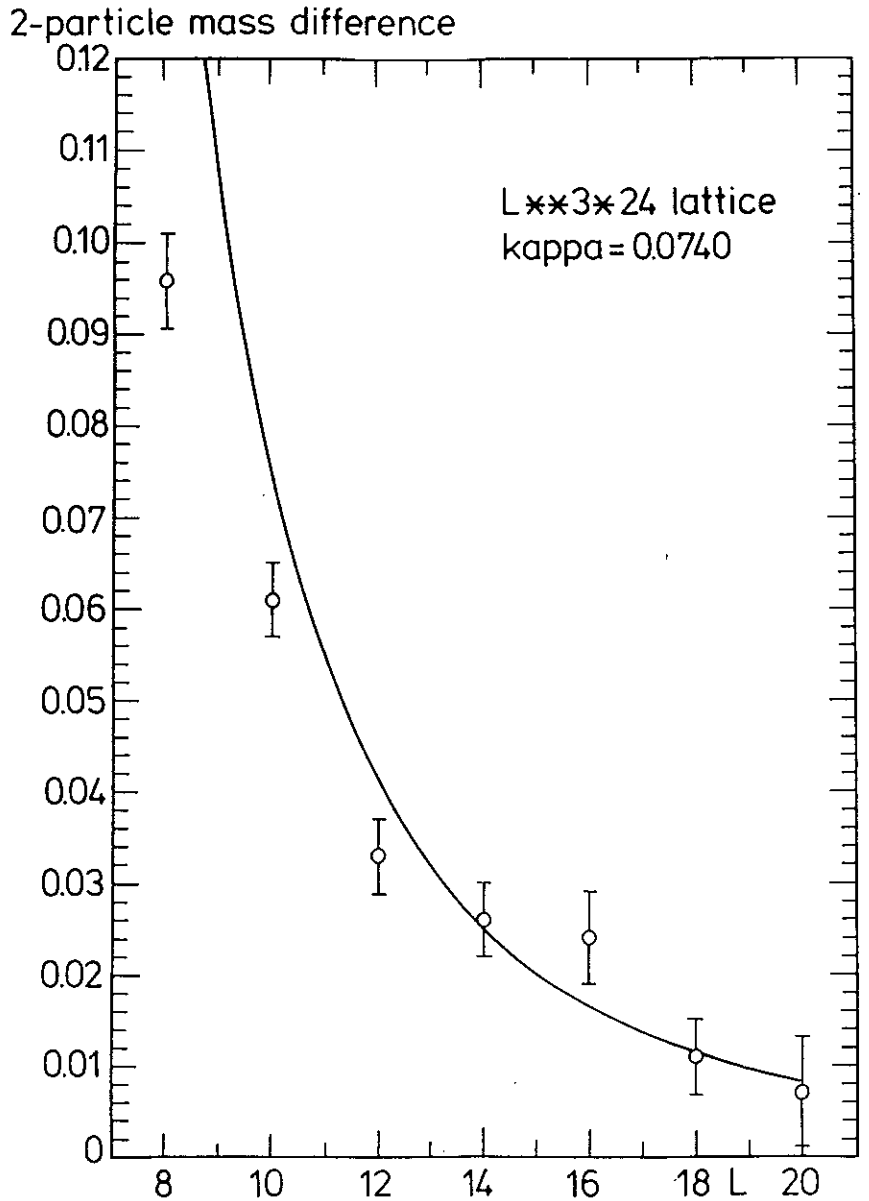
2-particle mass difference
0.12
0.11
0.10
0.09
0.08
0.07
0.06
0.05
0.04
0.03
0.02
0.01
0
L**3*24 lattice
kappa = 0.0740
8
10
12
14
16
18
L
20

Fig. 4 B